General Disclaimer

One or more of the Following Statements may affect this Document

- This document has been reproduced from the best copy furnished by the organizational source. It is being released in the interest of making available as much information as possible.

- This document may contain data, which exceeds the sheet parameters. It was furnished in this condition by the organizational source and is the best copy available.

- This document may contain tone-on-tone or color graphs, charts and/or pictures, which have been reproduced in black and white.

- This document is paginated as submitted by the original source.

- Portions of this document are not fully legible due to the historical nature of some of the material. However, it is the best reproduction available from the original submission.

CYCLES TILL FAILURE OF SILVER-ZINC CELLS WITH COMPETING FAILURES MODES—PRELIMINARY DATA ANALYSIS

Steven M. Sidik, Harold F. Leibecki,
and John M. Bozek
Lewis Research Center
Cleveland, Ohio

NASA

CYCLES TILL FAILURE OF SILVER-ZINC CELLS WITH COMPETING FAILURE

MODES - PRELIMINARY DATA ANALYSIS

by Steven M. Sidik, Harold F. Leibecki, and John M. Bozek

National Aeronautics and Space Administration
Lewis Research Center
Cleveland, Ohio 44135

INTRODUCTION

The silver/zinc electrochemical couple has found many applications. Mainly, its use in the past has been limited to primary applications requiring high currents, low weight, and permitted limited charge/discharge capabilities. With the advent of space probes and orbital spacecraft, secondary applications also became important. These applications require high specific energy and charge/discharge cycle life but permit limited current capability. A sealed secondary silver/zinc cell was developed for this reason (ref. 1). This cell used an inorganic/organic (I/O) separator and was very successful in the laboratory (refs. 2, 3, and 4). It was rated at 40 ampere hours (Ah), delivered 88 w-hr/kg (40 w-hr/pound) and about 400 cycles at a 40 percent depth of discharge (refs. 3 and 4).

Some near earth orbit missions motivated the development of a 12 Ah version of this cell. The specifications of this cell are:

    12 Ah rated sealed cell
    Pressed silver powder positive electrodes
    Pressed zinc oxide powder negative electrodes
    I/O Bag Separator around both electrodes
    Three negative electrodes
    Four positive electrodes
    45 weight percent KOH electrolyte
    Size:
            12.0 cm high to top of case
             6.0 cm wide
             2.25 cm thick
              316 gm weight

The specific energy of this cell was judged superior to that of other candidate electro-chemical couples (such as Ni/Cd, Ag/Cd) since the Ag/Zn couple is the most active. The theoretical specific energy of the silver-zinc cell is 440 w-hrs/kg, of the nickel-cadmium cell is 210 w-hrs/kg and of the silver-cadmium cell is 270 w-hrs/kg. It remained, therefore, to characterize the charge/discharge cycle life of this silver-zinc cell.

An experiment was designed which would serve two purposes. The primary objective of the experiment was to characterize the cycle life performance as a function of five variables (use conditions). These five variables are

> Charge rate (CR)
> Discharge rate (DR)
> Depth of discharge (DOD)
> Ambient temperature (T)
> End of charge voltage (ECV)

A second objective of the experiment is to estimate the variability of cycle life among cells tested under nominally the same conditions.

This report will first present a discussion of the variables considered and the experimental design. The design is a variation of a central composite factorial design commonly used in response surface methodology (ref. 5).

We then turn to fitting cycle life as a second order polynomial function of the five variables and conclusions that can be drawn from this fit. It will be shown that the primary results are the strong effect of depth of discharge (DOD) on cycle life and that cycle life peaks at about 25° to 30° C ambient temperature.

In the following section we differentiate between the two primary failure modes, shorting and low voltage. We first describe a competing failure modes model and estimation procedure (refs. 6 and 7). We then present equations which predict cycle life until a short develops if a low voltage cannot occur and cycle life until a low voltage failure if a short cannot occur. Whether a battery first fails by low voltage or shorting is determined primarily by temperature. At the lower temperatures the cells fail by low voltage and yield low cycle lives. At the highest temperatures the cells fail by shorting and yield low cycle lives. At intermediate temperatures we observe a mix of failure modes and higher cycle lives.

EXPERIMENT DESCRIPTION

Experiment Design

For this program, a total of 129 cells were tested. All were constructed from nominally identical materials by nominally identical methods. The five independent variables and the ranges over which they were investigated are

Charge rate (CR)	0.375 to 1.625 amperes
Discharge rate (DR)	1.25 to 5.00 amperes
Depth of Discharge (DOD)	20% to 100% of rated Ah
Temperature (T)	0° C to 40° C
End of Charge Voltage (E CV)	1.98 volts per cell to 2.02 volts per cell

The particular combinations of levels of these variables were chosen as a variation on central composite factorial designs (ref. 5). Table I provides the data for each cell tested. The test conditions are given in columns 2-6, the cycles to failure in columns 12-15, and mode of failure in column 16.

In this experiment one power supply unit was used to cycle a number of cells connected in series at the same charge rate and the same discharge rate. Nine combinations of charge and discharge rate were investigated. These levels are given in Table II. Each combination required a separate power supply unit.

Within each combination of these levels a full 2^3 factorial with 3 center point replicates was run with respect to DOD, T, and ECV. The specific levels are given in Table III. In addition to these runs, the axial points of a 2^3 central composite design on DOD, T, and ECV were run on power supply units 2, 4, 5, 6, and 8. The specific levels are also given in Table III.

These tests were performed by the Naval Weapons Support Center, Crane, Indiana.

Formation and Cycling Procedure

Before subjecting the cells to cycling under their respective test conditions, each cell was put through a pre-test formation and capacity check. This involved two charge/discharge cycles at room ambient temperature. Each cell was charged at 0.27 amps to 1.98-2.00 volts or 13.5 A-H whichever occurred first. Then each cell was discharged at 1.13 amps to 1.3 volts followed by a drain at 0.377 amps to 1.3 volts. This charge/ discharge sequence was followed twice. The ampere-hours in and out of the cell on each of these charges and discharges were recorded. For purposes of later analysis, the capacity (A-H) removed from the cells at the 1.13 amp and 0.377 amp rates were added and simply called capacity. Also for purposes of later analysis, the capacity removed for both formation cycles was averaged and is reported in Table I as actual capacity $(A-H_{actual})$.

After this formation the cells were ready for life cycling tests. Life cycling consists of discharging at the stated DR until the Amperehours out of the cell equals $(DOD_{nom})(12)/100$. If the cell cannot supply this at a voltage of 1.3 volts per cell or more, we say a low voltage failure occurs at that point. After discharge, the cells are charged at the stated CR until the voltage across the cells reaches ECV. If this takes more than twice the time it should at the stated charge rate we say a failure occurs. From the charge/discharge voltage behavior and the ability of a cell to hold a charge it is evident when a cell has developed an internal short. A cell may, therefore, fail by one of two modes, low voltage or shorting.

The complete cycling till failure process is as follows. After the formation, cells are cycled until a failure condition occurs. If this failure condition is a short, testing terminates and the cycle at which this occurs is denoted f_1 (in Table I). If this first failure condition is a low voltage condition, the cycle is noted as f_1 in Table I for that cell but charging and discharging continue as planned until the second failure condition occurs. If this second failure condition is a short the cycle at which it occurs is denoted f_2 in Table I and further testing is terminated. If this second failure condition is another low voltage condition, the cycle at which it occurs is denoted f_2 in Table I. The cell is then reformed once according to the formation criteria of voltage and current outlined previously.

After this reforming, cycling is continued until a third failure condition is encountered. If this is a short the cycle is recorded as f_3 in Table I, and testing terminates, while if it is a low voltage condition we note the cycle as f_3 in Table I and continue cycling as planned. The fourth failure condition is denoted as f_4 in Table I and terminates life cycling.

Since shorting terminates testing whenever it occurs, there are no further cycle lives reported in Table I after a short occurs. Reforming of the cells takes place only after cycle f_2.

ANALYSIS OF OVERALL CYCLE LIFE

In this section we consider life (number of cycles till failure) as a response regardless of the failure mode. In the following section we differentiate between the two modes of failure and describe equations for predicting the number of cycles until a cell fails by one mode under the condition the other mode is inoperative.

The five independent variables we use for life prediction are:

ξ_1 = charge rate (CR in amps)

ξ_2 = discharge rate (DR in amps)

ξ_3 = depth of discharge (DOD in %)

ξ_4 = ambient temperature (T in $^{\circ}$C)

ξ_5 = end of charge voltage (ECV in volts)

In terms of these variables, characterising cell performance is equivalent to providing an equation predicting cycles till failure as a function of $\xi_1, \ldots, \xi_5$. Rather than do this directly we define scaled variables (as is common in response surface methodology (ref. 5)) for the jth observation as

$$X_{1j} = (\xi_{1j} - 1.0)/0.625$$

$$X_{2j} = (\xi_{2j} - 3.13)/1.87$$

$$X_{3j} = (\xi_{3j} - 67.2)/19.4 \tag{1}$$

$$X_{4j} = (\xi_{4j} - 20)/10$$

$$X_{5j} = (\xi_{5j} - 2.00)/0.01$$

For X_1, X_2, X_4, X_5 the center point value is subtracted and the increment from the center point to the high level is used as the divisor. For X_3, the nominal depth of discharge (DOD_{nom}) as indicated in Table I is not used but the actual depth as calculated from the actual capacity based upon the formation cycles is. That is,

$$\xi_3 = \frac{12 \ DOD_{nom}}{A - H_{actual}} \tag{2}$$

For X_3, the center point of 67.2 is the average of ξ_3 while the scaling factor of 19.4 is the standard deviation of ξ_3.

The nominal DOD is the value a designer might use for design or mission analysis purposes where the actual capacity and actual DOD are generally unknown. But, once the actual cell is on hand and put through a capacity check, its actual capacity and hence actual DOD may be determined for predictive purposes.

As the response variable we use $Y_j = Y_j(X_1, \ldots, X_5)$ which may be cycles till failure (f_1, f_2, f_3, or f_4) or some function of cycles till failure (e.g., $\log f_1$).

The candidate function chosen as a starting point of analysis is simply a second order polynomial as commonly used in response surface methodology. That is, the statistical model is

$$Y_j = \beta_o + \beta_1 X_{1j} + \cdots + \beta_5 X_{5j}$$
$$+ \beta_{11} X_{1j}^2$$
$$+ \beta_{12} X_{1j} X_{2j} + \beta_{22} X_{2j}^2 \tag{3}$$
$$\vdots$$
$$+ \beta_{15} X_{1j} X_{5j} + \cdots + \beta_{55} X_{5j}^2 + \varepsilon$$

where ε is a random error with zero mean and constant variance σ^2 and the β's are unknown coefficients to be evaluated empirically.

As the response variable we chose to use $y = \log_{10}(\text{cycles})$. This choice was first made by analysis of residuals from fitting using $y = \text{cycles}$ and supported by probability plots of the residuals using $y = \log_{10}(\text{cycles})$.

For each cell there are up to four failure cycles (depending upon when a short occurs). For purpose of analysis, if a cell failed by shorting before cycle f_4, we simply repeat the last observed failure cycle for all succeeding failures. For example, cell number 626 failed first by the low voltage mode at cycle 74 and then failed by shorting at cycle 75 (see Table I). For a shorted cell, reconditioning is not possible and we simply use 75 for f_3 and f_4. There would be a qualitative difference between a cell which shorted at cycle 75 before ever failing by low voltage and say a cell which failed by low voltage twice before finally failing by shorting at cycle 75. This would not cause any serious distortion in modeling f_3 failures since the fact still remains that both cells failed by the 75th cycle.

Two cycle life predictive equations were fit, one to predict the f_2 failure cycle and the other to predict the f_4 failure cycle. The rationale for this is as follows. When the cell has a low voltage condition at cycle f_1 that indicates an inability to meet mission specifications for that cycle. Yet, it is possible to obtain more cycles which meet specs after that and indeed, Table I shows this to happen in almost every low voltage situation. Essentially, this is because low voltage failure is a slow degradation phenomenon and it is difficult to pinpoint a precise point of failure. Calling f_2 the life of a cell is a somewhat arbitrary attempt at defining such a point of failure. The cells are then reconditioned and again tested till "failure" which we will consider to be cycle f_4. The first equation, then attempts to predict useful cycle life if reforming cannot be done while the second equation attempts to predict useful cycle life if up to one reformation is permitted.

Cells number 618 and 727 were not included for analysis since they failed due to different causes (i.e., cell 618 failed due to operator error and 727 failed when its case ruptured).

Variable X_5 (measuring the effect of ECV) had no significant main effect or interaction with any variable in any of the analyses performed and is not included in any further discussion or analysis. (This lack of significance is probably due to the restricted range over which ECV was varied).

Table IV provides the summary statistics and estimated coefficients of equation (3) for the f_2 cycle life. The first column identifies the coefficient of equation (3) whose estimate is being reported. The second column gives the estimated coefficients (estimated by linear least squares regression analysis) and the estimated standard errors of the coefficients enclosed in parentheses. Those coefficient estimates significantly different from zero at the five percent significance level are indicated by an asterisk. The standard errors and significance level are determined by pooling both the pure replication and the lack of fit errors. At the bottom of the table are given the number of data points used in the fitting ($n = 127$), the standard error of estimate ($S = 0.342$) and the multiple correlation coefficient squared

($R^2 = 0.789$). The third column of Table V gives the estimates and standard errors of the coefficients when the data is refitted using only those coefficients significant at the five percent level of significance (i.e., reduced model). The standard error of estimate ($S = 0.348$) and squared correlation coefficient ($R^2 = 0.771$) indicate that the two equations fit the data essentially identically and will provide very nearly equal predictions.

Both model equations indicate that there are only two significant interactions among the variables (the interaction between charge rate and depth of discharge and the interaction between discharge rate and temperature). The interaction between discharge rate and temperature means that the particular effect temperature has on the cycle life of a cell is dependent upon the rate at which it is discharged.

Table V gives the corresponding information for the f_4 failure. Comparison of Tables IV and V shows very little difference either qualitatively or quantitatively between the fitted equations. The only appreciable difference is a lower standard error of estimate reported in Table V.

These equations and data were examined for indications of lack-of-fit or spurious observations by examining various residual and probability plots. On the basis of these it seemed that the results of cells 722 and 726 did not fit the patterns. Similar probability and residual plots discussed in the next section also indicated that cells 602 and 608 were not consistent with the rest of the data. Thus, equation (3) was refit to the 123 cells remaining after deleting from the analysis cells 602, 608, 722, and 726. The fitted constants for equation (3) and summary statistics for f_2 failures are given in Table VI and the results for f_4 failures in Table VII. Comparison of the full equations using 127 cells as opposed to 123 cells show the equations to have quite similar coefficient estimates. When comparing the reduced versions of the equations (i.e., all coefficients significant at the five percent level) there are minor differences in the second order terms. Specifically, for f_2 failures (Tables IV and VI) the X_2^2, X_3^2, and X_1X_4 terms are different. For f_4 failures (Tables V and VII) the X_1X_4 interaction appears in the 123 cell fit but not in the 127 cell fit. For the terms which appear in both full equations the coefficients are very similar in magnitude. The major changes are in the degree of fit as evidenced by the smaller standard error of estimate and larger R^2 values for the edited data set (i.e., the data set containing only 123 points).

We examine the fitted response surfaces in two ways. First, we perform a canonical analysis of the full second order equation. Second, we provide several parametric plots of life versus the independent variables.

In a canonical analysis of a second order polynomial response surface we first determine the stationary point of the surface and second perform a rotation of axes about that stationary point to new independent variables. In this process we let $\vec{X}_S$ denote the stationary point, Y_S denote the value of Y at that point, and $\vec{Z}$ denote the new (rotated) axes. (For details and further descriptions of this type analysis see ref. 5.) This reduces equation (3) to

the form of equation (4)

$$Y - Y_s = \lambda_1 z_1^2 + \cdots + \lambda_p z_p^2 \tag{4}$$

where the λ_i are the eigenvalues of the matrix of second order coefficients. The z_i variables are the axes of symmetry and are given by

$$z_1 = e_{11}(X_1 - X_{1s}) + \cdots + e_{1p}(X_p - X_{ps}) \tag{5}$$

where the e_{ij} are components of the eignvectors of the matrix of second order coefficients.

Table VIII provides the parameters of interest in the canonical analysis for the f_2 cycle life and Table IX for the f_4 cycle life. In Table VIII the λ_i indicate that the response surface is a saddle-shaped one. The value $\lambda_1 = 0.057$ indicates a rising ridge type of structure with respect to the variable

$$z_1 = -0.21(X_1 + 4.67) + 0.18(X_2 + 2.50)$$
$$+ 0.95(X_3 - 0.50) + 0.16(X_4 + 1.17)$$

The primary component of this variable is X_3 (depth of discharge). The value $\lambda_4 = -0.274$ indicates a falling valley with respect to the variable

$$z_4 = -0.17(X_1 + 4.67) - 0.49(X_2 + 2.50)$$
$$- 0.09(X_3 - 0.50) + 0.85(X_4 + 1.17)$$

This new variable is primarily a combination of X_2 (discharge rate) and X_4 (temperature). (This arises from the X_2X_4 interaction which is large and significant as seen in Table VI.) The surface is almost constant with respect to variable z_2 and somewhat decreasing with variable z_3. Variable z_3 is given by

$$z_3 = -0.69(X_1 + 4.67) + 0.62(X_2 + 2.50)$$
$$- 0.30(X_3 - 0.50) + 0.19(X_4 + 1.17)$$

which is a combination of all four original variables.

The λ_i and e_i of Table IX are very similar to those of Table VIII. The stationary point is shifted more toward the center of the design. Thus, the basic shape of the response surface is the same but shifted in location slightly.

The shape of the surface may be easier to understand by looking at figures 1 through 5. In these figures we plot the predicted $\log_{10} f_2$ cycle life using the reduced equation of Table VI. Figure 1 plots f_2 versus DOD

for five different temperature values. For these plots CR is held constant at 1.0 amp and DR is held constant at 3.13 amp. This plot clearly shows the rising ridge structure with respect to temperature and DOD. Figure 2 plots f_2 versus DOD for three charge rates. The small interaction between CR and DOD shows a steeper loss of life with respect to DOD at the higher charge rates. The curves show that slower charging gives better cycle life. Figure 3 shows f_2 versus DOD at three discharge rates. There is no interaction between these variables and the conclusion to be drawn is that lower discharge rates give longer life. Figure 4 plots f_2 versus temperature at three different discharge rates. We see that maximal life is obtained at a temperature dependent on discharge rate. This implies that as the discharge rate required increases, the optimal temperature also rises. Figure 5 plots f_2 versus temperature at three different charge rates. The interaction between temperature and charge rate is not as pronounced as the interaction between temperature and discharge rate. For any given CR there is a temperature providing maximal life and this temperature increases as charge rate increases. The less pronounced interaction of figure 5 as opposed to figure 4 is shown by the three curves being more nearly parallel.

COMPETING FAILURE MODES ANALYSIS

In the preceeding section we developed equations for predicting failure cycle as a function of the test conditions (i.e., the independent variables). In this section we differentiate between the two failure modes low voltage and shorting. Before the cell is put on test we assume a random time until failure due to low voltage has a probability distribution $F^{(1)}(y_1; X)$ and independently a random time until failure due to shorting has a probability distribution $F^{(2)}(y_2; X)$. The actual life of the cell is the smaller of these two lifetimes. As the notation indicates, we allow the distributions $F^{(i)}(y_i; X)$ to depend upon the test conditons, X. Specifically, we assume that $F^{(i)} = F^{(i)}(y_i; \mu^{(i,j)}, \sigma^{(i)})$ where F is an extreme value distribution with location parameter $\mu^{(i,j)}$ and scale parameter $\sigma^{(i)}$. The location parameter is assumed to be related to the test conditions (similarly to eq. (3)) as

$$\mu^{(i,j)} = \beta_o^{(i)} + \beta_1^{(i)} X_{1j} + \cdots + \beta_5^{(i)} X_{5j}$$

$$+ \beta_{11}^{(i)} X_{1j}^2$$

$$+ \beta_{12}^{(i)} X_{1j}^2 X_{2j} + \beta_{22}^{(i)} X_j^2$$

$$+ \cdots$$

$$+ \beta_{15} X_{1j} X_{5j} + \cdots + \beta_{55}^{(i)} X_{5j}^2 \qquad (6)$$

For the smallest extreme value distributions

$$F(y; \mu, \sigma) = 1 - \exp\left\{-\exp\left(\frac{y-u}{\sigma}\right)\right\} \qquad (7)$$

(If life follows a Weibull distribution, then log life is known to follow a smallest extreme value distribution.) The observed data is of the form

$$
\begin{array}{cccc}
\text{life} & \text{mode} & \text{-----} & \text{test conditions} & \text{---}
\end{array}
$$

$$
\begin{bmatrix}
Y_1 & M_1 & X_{11} & \cdots & X_{1k} \\
\cdot & \cdot & \cdot & & \cdot \\
\cdot & \cdot & \cdot & & \cdot \\
\cdot & \cdot & \cdot & & \cdot \\
Y_n & M_n & X_{n1} & \cdots & X_{nk}
\end{bmatrix}
$$

We also critically examine the assumptions using probability plots and "residual" plots.

Methods for estimating the parameters (i.e., the β's and σ's) of these models and some simulation studies of the properties of these estimators is given in reference 7. The method used is maximum likelihood and this requires the solution of sets of non-linear equations. (The equations to be solved are given in the appendix.) The method of solution is straightforward but can be unstable if the model equation (eq. (6)) has too many terms which are insignificant. In an attempt to avoid this potential problem, we first separate the full set of data into two parts. The first part of the data is for cells that failed by low voltage and the second part for cells that shorted. Models of the form of equation (3) are then fit using ordinary least squares to each data set individually. This provides a first guess as to the form of the equation needed for each mode and also starting values for the β's and σ's required for the iterative maximum likelihood method.

As with ordinary multiple linear regression analysis, these models must be considered tentative in nature and examined for adequacy of fit and spurious observations. We present our results by discussing:

- The least squares fits to the short-only and low voltage-only data

- The corresponding maximum likelihood estimates

- Various "residual" plots for diagnosing adequacy of fit

- And the maximum likelihood estimates for the models and edited data sets

Analyses of All the Data

The data was split into sets of $n_1 = 97$ low voltage failures and $n_2 = 30$ short failures for a total of 127 data points. As discussed earlier, two cells (727 and 618) have been eliminated from the analysis. Table X presents the results of the linear regression analysis for cycle f_2 failures while Table XI presents the corresponding results for cycle f_4 failures. In each table we retain only those terms with coefficients significant of the five percent significance level except for the T and T^2 terms. For the short data there is a large correlation between T and T^2 when using the scaling of equations (1). It turns out that either one but not both of these terms are significant. We included both of those terms regardless of their individual significance levels. Tables X and XI do not require much discussion except to note that the values of the $\hat{\beta}$'s and σ's reported therein were used as starting values for the iterative maximum likelihood method.

In Table XII we present the maximum likelihood estimates of the coefficients for the f_2 failure cycle for each mode and their estimated standard errors in parentheses. Upon comparing Tables X and XII it may be seen that the coefficient estimates are not far apart except for a few instances. For the low voltage failures, the DR coefficients are somewhat different. For the short failures the individual coefficients of T and T^2 are somewhat different. For both modes the constant coefficients are larger by the maximum likelihood method than by the least squares method. Similar comments hold true for the f_4 failure results (reported in Table XIII) except that the X_1X_2 interaction has reversed signs for the short failure mode between Tables XI and XIII.

These fits were examined by "residual" plots as follows. For the separate least squares fits, standardized residuals were calculated in the standard manner (i.e., $(y - \hat{y}/s)$. These were plotted in various ways including versus each independent variable and versus the predicted value. Three of these plots are given in figure 6 through 8. Figure 6 presents the residuals against discharge rate for the cycle f_2 low voltage failure regression. There is some indication that the variance increases as DR increases and that there may be three outlying cells at the highest DR. (These are indicated by the $\bigcirc$ and 2 at the bottom right of the plot.) Two of these three are cells 722 and 726. Figure 7 presents residuals against scaled temperature for the cycle f_4 low voltage failure data. The two largest negative residuals are cells 722 and 726. There is also a large positive residual at the lowest temperature. Figure 8 plots the residuals versus the predicted values for the cycle f_4 low voltage failure regression. It almost appears as if there are two populations of residuals. The lowest predicted values are over-predicted while the residuals tend toward more uniform behavior as $\hat{y}$ increases. This probably indicates some sort of flaw in the model equation. One problem with the model as used here is that for the very low cycle lives, $\log_{10}$ (cycles) cannot be well described by any continuous distribution, such as the extreme-value or normal. The greatest number of cells had much larger lifetimes, however, and this is where we are most interested in battery performance anyhow. The only action taken at this point was to delete cells 722 and 726 from analysis.

From the equations estimated by maximum likelihood and presented in Tables XII and XIII we computed "residuals" as follows. We first compute $\hat{\mu}(x)$ the predicted location parameter for the mode by which that cell failed. The residual is then defined as $y_i - \hat{\mu}$. This is an expedient but not necessarily correct approach and may lead to some distortion where there is considerable overlap of the distributions of the two failure modes. Various plots of these residuals were examined and three of these are given as figures 9 through 11. Figure 9 plots the residuals versus scaled charge rate for the cycle f_4 short failures. The two large negative residuals at the lowest charge rate are cells 602 and 608.

In figure 10 we provide a probability plot of the residuals on an extreme value probability scale while figure 11 gives a probability plot on a normal probability scale. These are for the cycle f_4 short failures. It is quite clear that the residuals fit an extreme value distribution much better than a normal distribution. The only action taken at this point was to delete the data from cells 602 and 608 from the analysis.

Analysis of Edited Data

The data were re-analyzed by the same techniques described in the previous sections except with the data from cells 602, 608, 722, and 726 removed. Equation (3) was fit to the 95 low voltage failures and the 28 short failures separately with the resulting least squares coefficients given in Tables XIV and XV. Comparing Table X which is for the unedited f_2 data to Table XIV which gives the fit for the edited f_2 data, it may be noted that there is very little difference between the coefficients. The fits seem somewhat improved as evidenced by the larger R^2 and smaller S values. Similar comments hold for the comparison of Tables XI and XV which present the f_4 regression results.

As before, the least squares results were used as initial values for the iterative maximum likelihood procedure. Table XVI gives the refined estimates for the f_2 failure times. In parentheses next to each coefficient estimate are given their estimated standard errors. Comparing Tables XII and XVI we see that the charges in coefficient estimates are minor except for the individual coefficients of T and T^2 for the shorting mode equations. Comparing Tables XIII and XVII which give the maximum likelihood estimates for the f_4 cycle life, the differences are again all small except for the individual coefficients on T and T^2 and the reversal in sign of the DR x CR interaction. The sign and magnitude of the DR x CR interaction in Table XVII are consistent with the least squares results.

It may be noted that in Tables XVI and XVII there are several coefficient estimates which are within one estimated standard error of zero (e.g., the f_2 DR low voltage and f_2 DOD^2 short coefficients of Table XVI). One is tempted to compute a t-like statistic and conclude these terms are not significant This may not be true because correlations among the $\hat{\sigma}$ and $\hat{\beta}$ estimates may lead to a very skewed distribution of the t-ratio in some instances (ref. 8). We have refitted the maximum likelihood estimates for reduced models but these are not presented or discussed in this report. It turns out that the coefficients of Tables XVI and XVII provide the lowest (most conservative) estimator

for life. For this reason we use these equations to compare the effects of the independent variables on the life by each mode. Figures 12 through 16 provide some of the more interesting plots of predicted life times.

For a smallest extreme value distribution with location parameter μ and scale parameter σ, the expected life is $\mu - \gamma\sigma$ where $\gamma = 0.5776$ is Eulers constant. For the following plots, we use as expected life $\hat{\mu}(X_1, \cdots, X_5) - \gamma\hat{\sigma}$.

Figure 12 plots expected (log life f_2) versus temperature for three different discharge rates. For these, charge rate is held at 1.0 amp, DOD at 67.2 percent of actual capacity and E CV limit at 2.00 volts. The curves for low voltage failure cycle indicate initially rising life with temperature. There is a maximum with respect to temperature and the maximizing temperature depends upon discharge rate. The higher the temperature and discharge rate, the more cycles before a low voltage failure occurs. The curves for short life indicate that as temperature increases, shorts develop sooner and that shorts develop sooner at the low discharge rates. At about 25° to 30° C is the crossover between failure modes. At the lowest temperatures the cells fail by low voltage long before shorts have had a chance to develop. At 40° C, the cells are developing shorts before they have the chance to fail by low voltage. One implication of the reversed behavior of life with respect to temperature is that if a change could be made to the cell which prevented low voltage failures from occurring at temperatures of say 10° C but had no effect on shorts developing, then we could expect an increased life of approximately 400 cycles. It is not clear that such changes could be made. Certainly, more effort should be expended on post-mortem analyses of cells to break down cause of failure into more directly assignable causes than low voltage and short.

Figure 13 plots expected ($\log_{10}$ life f_2) versus depth of discharge for several different temperatures. For these, charge rate was held at 1.0 amp, discharge rate was held at 3.13 amp, and EOCV limit at 2.00 volts. The plots show that expected life decreases with depth of discharge but at slightly different rates. The dependence of failure mode on temperature is clearly evident also.

Figure 14 plots $\log_{10}$ (life f_2) versus DOD for various charge rates. For these, temperature is held at 20° C, discharge rate at 3.13 amps, and E CV limit at 2.00 volts. For the low voltage failure mode, expected life is decreasing with DOD and, at these conditions, is the dominant failure mode regardless of charge rate. For the shorting failure mode, expected life decreases with DOD at the higher charge rates while it essentially remains constant at the lower charge rates.

Figure 15 plots $\log_{10}$ (life f_2) versus DOD for various discharge rates. For these, charge rate is held at 1.0 amp, temperature at 20° C and E CV limit at 2.00 volts. For the low voltage failures, there is little effect on life from discharge rate but expected life is decreasing with DOD. For the shorting mode expected $\log_{10}$ (f_2) decreases with DOD at the low discharge rates but decreases less at the higher discharge rates. As in figure 14, the dominating failure mode is low voltage at those conditions.

Figure 16 plots expected cycles till f_2 failure for three charge rates. It is similar in shape to figure 12 which plots expected cycles till f_2 failure for three discharge rates. Figure 16 shows that at low temperatures low voltage is the dominating failure mode while at high temperatures shorting is the dominating failure mode.

DISCUSSION

In this section we discuss the effects of each of the independent variables, the results of the regression on overall life and their interpretation, the results of the competing failure mode modal and analysis, and recommendations for further research.

There are numerous factors which could affect the cycling life of a cell but the five we considered are primarily those that define the use environment of the cell. Their levels and ranges of variation were chosen on the basis of what was anticipated to effect cycle life at the time the experiment was designed.

Charge and Discharge Rates

Variations in charge and discharge rates have an effect on life for several reasons. Either rate may have an effect on the crystal structure of the active materials which may in turn affect the rates at which the electrochemical couple progresses. High charge rates may have accelerated zinc dendrite growth leading to early shorting (ref. 9). In fact, figures 2 and 5 show that overall life decreases as the charge rate increases. Figure 3 shows that at $T = 20^o$ C the overall life decreases as DR increases. Figure 4 shows that at low temperatures overall life decreases with DR while it increases with DR at higher temperatures. Figure 12 indicates the effects by mode. That is, at the lowest temperatures, the dominating failure mode is low voltage and the effect of DR on low voltage life is mixed. At the higher temperatures, the dominating failure mode is shorting and shorts develop in fewer cycles at the lower discharge rates.

Figure 5 shows that overall life decreases as CR increases. Figure 16 shows this to be true for each mode. It is interesting that decreasing the discharge rate promotes early shorting while increasing charge rate promotes early shorting. Thus, the data indicates slow charging and rapid discharging are best in terms of shorting.

Depth of Discharge

Variations in the depth of discharge require different percentages of the active materials to be exercised during each cycle. Since the reactions are never totally reversible, high DOD should lead to decreased cycle life. In fact, figure 1 shows a large decrease in overall cycle life. Figures 13, 14, and 15 also show that both low voltage and shorting lifetimes generally decrease as DOD increases. At the lowest charge rates and the highest discharge rates there is little or no decrease in cycle life as DOD increases.

Care must be taken in drawing conclusions at conditions other than specified in the figures due to the interactions among the variables.

Temperature

Rates of chemical reactions depend strongly upon temperature and hence cycle life of a cell should depend strongly on the temperature. Changes in temperature may effect the crystal growth, charge acceptance, growth of dendrites, or dissolution of cell separator components. Figures 4 and 5 show the effect of temperature on overall cycle life. For each charge and discharge rate combination there is some optimal temperature. Figures 12 and 16 show the mode of failure depends strongly on the temperature. High temperatures promote processes that lead to shorting while at low temperatures shorts are slow to develop.

The rate of zinc dendrite propagation increases as the concentration of the zincate ions increases while the initiation time for dendrite formation decreases with increasing over-potential, temperature and zincate concentration (ref. 9). At low temperature, the diffusion of zincate is less than at the higher temperatures and would cause a mean transport conditions conducive to the results observed.

End of Charge Voltage

It was felt that E CV might effect cycle life primarily due to the possibility of gassing at high end of charge voltages. In this experiment we found no evidence of an effect of E CV over the range examined. It is possible that we did not investigate a large enough range.

Life Prediction Models

For mission analysis and component design purposes, the analyst is primarily interested in knowing what cycle life might be expected under the conditions at which the cell might be used. In general, the mode of failure is unimportant. (This is to some extent not true because failure by low voltage is not a well-defined condition. For most missions a short failure may be considered to be terminal whereas if low voltage failures occur, the mission might be extended if the cell is reformed.) The equations of Tables VI and VII provide predictive equations for overall failure by our definitions of failure. The reliability of the equations as a predictive tool are partially indicated by the estimated standard deviations which imply that the uncertainty in a further predicted $\log_{10} (f_2)$ is $S = 0.300$.

Plus and minus two standard error prediction limits in $\log_{10} (f_2)$ of $2S = 0.60$ translate to error limits of $f_2 \times 1 \quad 2\hat{o}$ or from $0.25 f_2$ to $3.98 f_2$. For the f_4 failure equation we have $S = 0.248$ which leads to proportional error limits of from $0.32 f_4$ to $3.13 f_4$. That is, we can predict cycle life to within a factor of 3 or 4.

For the battery researcher, the competing failure mode model and
analysis provide considerable more information for improving cell cycle
life. In this study we have simplified the category of failure into two
classes of failure, namely low voltage and shorting. This is recognized
as a simplification since there may be several places and causes for
either type of failure. Ideally, each cell should undergo a post-mortem
analysis to further differentiate failure causes. The competing failure
modes analysis does provide a first attempt at separating causes and an
indication of which design changes might be most important to consider.
For instance, figure 12 shows that at a temperature of 0° C and DR of
1.0 amp a cell will yield about four cycles before a low voltage fail-
ure. If a design change could be utilized which alleviated this type of
failure but would not affect the formation of shorts, we could expect to
get about 500 cycles before shorting would terminate cell life. Of
course, such changes may also adversely affect cycle life due to shorting.
The independence of the two failure modes assumed in the model could be
a restrictive assumption. However, the use of the competing failure
mode model analysis along with post-mortem analysis of the cells
promises to be a useful and informative tool.

APPENDIX

MAXIMUM LIKELIHOOD ESTIMATE EQUATIONS

Assume that an experiment is performed in which I items are life tested at varying combinations of J stress variables and that the design is specified by the design matrix

$$Z = \begin{bmatrix} z_{11} & \cdots & z_{1J} \\ \cdot & & \cdot \\ \cdot & & \cdot \\ \cdot & & \cdot \\ z_{11} & \cdots & z_{1J} \end{bmatrix} \tag{A-1}$$

The response observed for each item is a lifetime y_i $(i = 1, I)$ and the mode by which the item failed, m_i. The number of modes by which the item might fail is denoted M.

We assume that for observation i and mode m the cumulative distribution function of time until failure is defined by

$$F_i^{(m)}\left[y; \mu_i^{(m)}, \sigma^{(m)}\right] = 1 - \exp\left\{-\exp\left[\frac{y - \mu_i^{(m)}}{\sigma^{(m)}}\right]\right\} \tag{A-2}$$

where

$$\mu_i^{(m)} = \beta_1^{(m)} z_{i1} + \cdots + \beta_J^{(m)} z_{iJ} \tag{A-3}$$

The probability density function is given by

$$f_i^{(m)}\left[y; \mu_i^{(m)}, \sigma^{(m)}\right] = \frac{1}{\sigma^{(m)}} \exp\left\{\frac{y - \mu_i^{(m)}}{\sigma^{(m)}} - \exp\left[\frac{y - \mu_i^{(m)}}{\sigma^{(m)}}\right]\right\} \tag{A-4}$$

In general we will not necessarily have

$$\sigma^{(m)} = \sigma^{(m')} \qquad \text{for} \quad m \neq m' \tag{A-5}$$

nor

$$\beta_j^{(m)} \ne \beta_j^{(m')} \qquad \text{for} \quad m \ne m' \tag{A-6}$$

That is, we do not a priori assume any of the failure modes to have parameter values in common.

It may be shown that the natural logarithm of the likelihood function is

$$\ln L = \sum_{i=1}^{I} \ln \left\{ f_i^{(m_i)} \prod_{m \ne m_i} \left[1 - F_i^{(m)} \right] \right\} \tag{A-7}$$

is obtained where

$$\ln L = \ln L \left[\beta_1^{(1)}, \ldots, \beta_J^{(1)}, \beta_1^{(2)}, \ldots, \beta_J^{(2)}, \ldots, \right.$$

$$\left. \beta_1^{(M)}, \ldots, \beta_J^{(M)}, \sigma^{(1)}, \ldots, \sigma^{(M)}; y_1, \ldots, y_I \right] \tag{A-8}$$

To obtain maximum likelihood estimators, the standard method (assuming it works) is to solve the system of JM (nonlinear) equations

$$\left. \begin{array}{ll} \dfrac{\partial \ln L}{\partial \beta_1^{(m)}} = 0 & (m = 1, M) \\[2em] \quad \cdot \\ \quad \cdot \\ \quad \cdot \\ \dfrac{\partial \ln L}{\partial \beta_J^{(m)}} = 0 & (m = 1, M) \\[2em] \dfrac{\partial \ln L}{\partial \sigma^{(m)}} = 0 & (m = 1, M) \end{array} \right\} \tag{A-9}$$

If the different failure modes have no parameters in common, as will generally be true by equations (A-5) and (A-6), this system of JM equations splits into M separate systems of J equations which may be independently solved. In particular, the mth system reduces to

$$0 = \sum_{\substack{\text{mode m} \\ \text{failures}}} \frac{\partial}{\partial \beta_1^{(m)}} \ln f_i^{(m)} + \sum_{\substack{\text{other mode} \\ \text{failures}}} \frac{\partial}{\partial \beta_J^{(m)}} \ln \left[1 - F_i^{(m)} \right]$$

$$\vdots$$

$$0 = \sum_{\substack{\text{mode m} \\ \text{failures}}} \frac{\partial}{\partial \beta_J^{(m)}} \ln f_i^{(m)} + \sum_{\substack{\text{other mode} \\ \text{failures}}} \frac{\partial}{\partial \beta_J^{(m)}} \ln \left[1 - F_i^{(m)} \right] \qquad \text{(A-10)}$$

$$0 = \sum_{\substack{\text{mode m} \\ \text{failures}}} \frac{\partial}{\partial \sigma^{(m)}} \ln f_i^{(m)} \quad \sum_{\substack{\text{other mode} \\ \text{failures}}} \frac{\partial}{\partial \sigma^{(m)}} \ln \left[1 - F_i^{(m)} \right]$$

From equations (A-3) and (A-4) it may be shown these equations reduce to

$$\frac{1}{\sigma} \sum_{\substack{\text{failed by} \\ \text{mode}}} z_{ij} - \frac{1}{\sigma} \sum_{\substack{\text{all} \\ \text{failures}}} z_{ij} \exp \left(\frac{y_i - \Sigma \beta_k z_{ik}}{\sigma} \right) = 0 \qquad (j = 1, J)$$

$$\frac{1}{\sigma^2} \sum_{\substack{\text{failed by} \\ \text{mode}}} (y_i - \Sigma \beta_k z_{ik} + \sigma) - \frac{1}{\sigma^2} \sum_{\substack{\text{all} \\ \text{failures}}} (y_k - \Sigma \beta_k z_{ik}) \exp \left(\frac{y_i - \Sigma \beta_k z_{ik}}{\sigma} \right) = 0$$

$$\text{(A-11)}$$

These nonlinear equations have no closed-form solution but may be solved by several iterative methods.

It is well-known that, under appropriate regularity conditions, maximum likelihood estimators (MLE) are consistent and asymptotically normally distributed. It is also known for the Weibull and extreme value distributions that the minimal sufficient statistics are the trivial ones consisting of the order statistics. It thus becomes of considerable interest to determine how rapidly the MLE's approach their asymptotic unbiasedness and covariance structure. The asymptotic covariance structure and the Cramer-Rao lower bound are defined by the inverse of the Fisher information matrix (ref. 10, p. 194).

For the model considered in this report the Fisher information matrix is the block-diagonal matrix

$$
\begin{bmatrix}
I^{(1)} & 0 & \cdots & & 0 \\
0 & I^{(2)} & & & \\
\vdots & \vdots & & & \\
0 & 0 & \cdots & & I^{(M)}
\end{bmatrix}
\tag{A-12}
$$

where

$$
-I^{(m)} = E
\begin{bmatrix}
\dfrac{\partial^2 \ln L}{\partial\left[\beta_1^{(m)}\right]^2} & \cdots & \cdots & \dfrac{\partial^2 \ln L}{\partial\beta_1^{(m)}\partial\sigma^{(m)}} \\
\vdots & & \vdots & \vdots \\
\cdots & \cdots & \dfrac{\partial^2 \ln L}{\partial\left[\beta_J^{(m)}\right]^2} & \dfrac{\partial^2 \ln L}{\partial\beta_J^{(m)}\partial\sigma^{(m)}} \\
\dfrac{\partial^2 \ln L}{\partial\beta^{(m)}\partial\sigma^{(m)}} & \cdots & \dfrac{\partial^2 \ln L}{\partial\beta^{(m)}\partial\sigma^{(m)}} & \dfrac{\partial^2 \ln L}{\partial\left[\sigma^{(m)}\right]^2}
\end{bmatrix}
\tag{A-13}
$$

These expressions are estimated as described in reference 6 and yield the estimated standard errors of the coefficients reported in Tables XII, XIII, XVI, and XVII.

REFERENCES

1. Himy, A. (1971). Development of a Heat-Sterilizable 40-Ah Sealed Silver-Zinc Cell. NASA CR-1812.

2. Bozek, John M. (1974). Structure and Function of an Inorganic-Organic Separator for Electrochemical Cells - Preliminary Study. NASA TM X-3080.

3. Smatko, J. S. (1974). Fabrication and Test of Inorganic/Organic Separators. SRI-PYU-2285, Stanford Research Inst., Memlo Park, Calif. (NASA CR-134646).

4. Lear, J. W., Donovan, R. L., and Imamura, M. S. (1978). Development of Single-Cell Protectors for Sealed Silver-Zinc Cells. MCR-78-571, Martin Marietta Corp., Denver, Col. (NASA CR-159407).

5. Myers, Raymond H. (1971). Response Surface Methodology. Alyn and Bacon, Boston.

6. Nelson, W. B. (1974). Analysis of Accelerated Life Test Data with a Mix of Failure Modes by Maximum Likelihood. Report 74CRD160, General Electric Company, Schenectady, N.Y.

7. Sidik, S. M. (1979). Maximum Likelihood Estimation for Life Distributions with Competing Failure Modes. NASA TM-79126.

8. Schmee, J., and Nelson, W. B. (1976). Confidence Limits for Parameters of (log) Normal Life Distributions from Small Singly Censored Samples by Maximum Likelihood. Report 76CRD218, General Electric Co., Schenectady, N.Y.

9. Fleischer, Arthur, Ed. (1971). Zinc-Silver Oxide Batteries. Wiley, N.Y.

10. Zacks, Shelemyahu (1971). The Theory of Statistical Inference. Wiley, N.Y.

TABLE I. — 12 AMP-HR SILVER-ZINC CHARACTERIZATION TEST

PACK NO.	CHARGE RATE AMPS	DISCHARGE RATE AMPS	DEPTH OF DISCHARGE %	TEST TEMP °C	END OF CHARGE VOLTS	ACTUAL FORMATION CAPACITY					CYCLES TO FAILURE				FAILURE MODE
						CHG#1 A-H	DCHG#1 A-H	CHG#2 A-H	DCHG#2 A-H	CHG#3 A-H	F1	F2	F3	F4	
601A	0.375	1.25	43.2	10	1.99	11.89	10.55	11.76	11.22	11.66	138	145	157	167	LV
602A	0.375	1.25	76.8	10	1.99	11.74	10.62	11.39	11.02	11.43	101	103	121	122	S
603A	0.375	1.25	43.2	30	1.99	12.61	11.71	11.71	11.13	12.27	246	247			S
604A	0.375	1.25	76.8	30	1.99	12.18	10.96	11.87	11.30	11.99	150	151			S
605A	0.375	1.25	43.2	10	2.01	12.29	11.55	12.25	11.60	12.42	187	201	240	241	LV
606A	0.375	1.25	76.8	10	2.01	12.45	11.21	11.26	10.85	12.02	76	7.	92	93	LV
607A	0.375	1.25	43.2	30	2.01	12.87	12.11	12.31	11.66	12.78	245	252			S
608A	0.375	1.25	76.8	30	2.01	13.18	11.96	11.79	10.47	12.05	86				S
609A	0.375	1.25	60.0	20	2.00	11.99	10.64	11.41	10.96	12.09	325	331	337	338	LV
610A	0.375	1.25	60.0	20	2.00	11.70	10.41	11.47	11.06	12.02	281	282	306	308	LV
611A	0.375	1.25	60.0	20	2.00	13.48	12.20	12.60	11.34	12.81	309	310	359	360	LV
612A	1.000	1.25	43.2	10	1.99	12.47	11.73	11.61	10.90	12.42	78	79	81		LV
613A	1.000	1.25	76.8	10	1.99	12.99	11.70	11.63	10.38	12.00	8				LV
614A	1.000	1.25	43.2	30	1.99	12.83	11.73	11.67	11.04	12.52	283	285	292	294	LV
615A	1.000	1.25	76.8	30	2.01	12.63	11.60	12.09	11.47	12.30	130	131			S
616A	1.000	1.25	43.2	10	2.01	12.29	11.43	11.15	10.54	11.88	79				LV
617A	1.000	1.25	7?.3	10	2.01	12.38	11.36	12.08	11.54	12.15	4	42	54	55	LV
618A	1.000	1.25	43.2	30	2.01	12.29	11.49	11.86	10.76	12.46	115				OP
619A	1.000	1.25	76.8	30	2.00	12.83	11.64	12.07	11.49	12.64	160	161	164	165	LV
620A	1.000	1.25	60.0	20	2.00	11.45	10.26	11.12	10.32	11.65	122	123	160	164	LV
621A	1.000	1.25	60.0	20	2.00	11.17	9.98	11.27	10.74	11.66	143	144	154	155	LV
622A	1.000	1.25	60.0	20	2.00	12.14	11.11	12.15	11.87	12.53	161	162	172	173	LV
623A	1.000	1.25	20.0	20	2.00	12.69	11.87	11.23	10.53	12.45	466	467			LV
624A	1.000	1.25	100.0	20	2.00	12.20	10.77	10.98	10.57	11.66	99	100	108	110	LV
625A	1.000	1.25	60.0	0	2.00	11.07	10.17	11.02	10.45	11.48	3	4	5	8	LV

TABLE I. - Continued. 12 AMP-HR SILVER-ZINC CHARACTERIZATION TEST

PACK NO.	CHARGE RATE AMPS	DISCHARGE RATE AMPS	DEPTH OF DISCHARGE %	TEST TEMP °C	END OF CHARGE VOLTS	CHG#1 A-H	DCHG#1 A-H	CHG#2 A-H	DCHG#2 A-H	CHG#3 A-H	F1	F2	F3	F4	FAILURE MODE
626A	1.000	1.25	60.0	40	2.00	10.81	10.51	11.24	10.87	11.85	74	75			S
627A	1.000	1.25	60.0	20	1.98	11.61	10.36	11.46	11.13	11.75	105	106	134	135	LV
628A	1.000	1.25	60.0	20	2.02	11.55	10.23	11.46	11.07	12.02	154	177	183	184	LV
629A	1.625	1.25	43.2	10	1.99	12.96	11.83	11.86	10.89	12.61	55	56	75	76	LV
630A	1.625	1.25	76.8	10	1.99	12.05	10.89	11.74	11.06	12.51	3	4	7	8	LV
631A	1.625	1.25	43.2	30	1.99	11.97	11.05	10.80	10.04	11.68	216	217			LV
632A	1.625	1.25	76.8	30	1.99	11.88	10.66	11.03	10.28	11.73	62	63	80	81	LV
633A	1.625	1.25	43.2	10	2.01	12.29	11.17	10.96	10.13	11.88	79	81	96	97	LV
634A	1.625	1.25	76.8	10	2.01	11.85	10.74	11.66	10.87	12.14	4	5	8	9	LV
635A	1.625	1.25	43.2	30	2.01	12.29	11.38	10.96	10.17	11.94	229	230	238	242	LV
636A	1.625	1.25	76.8	30	2.01	11.81	10.66	11.72	10.98	11.90	109	110	113	114	LV
637A	1.625	1.25	60.0	20	2.00	12.42	11.43	11.63	10.66	12.20	73	74	98	99	LV
638A	1.625	1.25	60.0	20	2.00	11.61	10.45	11.21	10.75	12.21	69	70	95	96	LV
639A	1.625	1.25	60.0	20	2.00	11.97	10.68	11.96	11.22	12.26	32	33	83	86	LV
640A	0.375	3.13	43.2	10	1.99	12.29	11.47	11.35	10.67	12.60	142	170	210	204	LV
641A	0.375	3.13	76.8	10	1.99	12.34	11.17	11.63	10.98	12.02	44	54	66	71	LV
642A	0.375	3.13	43.2	30	1.99	12.91	11.92	11.20	10.53	12.65	398	399			S
643A	0.375	3.13	76.8	30	1.99	11.23	10.00	10.99	10.66	11.15	314	315	318	319	LV
644A	0.375	3.13	43.2	10	2.01	11.61	10.81	11.48	10.88	12.31	108	109	172	176	LV
645A	0.375	3.13	76.8	10	2.01	12.16	10.55	11.33	10.92	11.95	52	53	70	71	LV
646A	0.375	3.13	43.2	30	2.01	12.44	11.22	11.48	10.85	12.11	286	287			S
647A	0.375	3.13	76.8	30	2.01	11.63	10.68	11.53	11.39	11.61	376	377			S
648A	0.375	3.13	60.0	20	2.00	12.08	10.79	11.64	10.98	12.15	179	180	214	219	LV
649A	0.375	3.13	60.0	20	2.00	11.91	10.62	11.08	10.19	11.16	170	171	219	221	LV
650A	0.375	3.13	60.0	20	2.00	10.62	9.44	10.60	9.83	10.75	245	250	275	281	LV

TABLE I. - Continued. 12 AMP-HR SILVER-ZINC CHARACTERIZATION TEST

PACK NO.	CHARGE RATE AMPS	DISCHARGE RATE AMPS	DEPTH OF DISCHARGE %	TEST TEMP °C	END OF CHARGE VOLTS	ACTUAL FORMATION CAPACITY CHG#1 A-H	DCHG#1 A-H	CHG#2 A-H	DCHG#2 A-H	CHG#3 A-H	CYCLES TO FAILURE F1	F2	F3	F4	FAILURE MODE
651A	0.375	3.13	20.0	20	2.00	13.20	11.96	11.57	10.34	11.85	527				S
652A	0.375	3.13	100.0	20	2.00	11.41	10.32	11.19	10.34	11.08	64	65	77	78	LV
653A	0.375	3.13	60.0	0	2.00	11.33	10.04	10.87	10.00	11.08	1	2	3	4	LV
654A	0.375	3.13	60.0	40	2.00	11.91	10.64	11.34	10.64	11.75	101	102			S
655A	0.375	3.13	60.0	20	1.98	11.61	10.23	11.31	11.04	11.72	197	198	217	218	LV
656A	0.375	3.13	60.0	20	2.02	11.62	10.23	10.13	9.83	10.29	200	203	216	217	LV
657A	1.000	3.13	43.2	10	1.99	11.77	10.68	11.61	10.90	11.93	33	38	56	69	LV
658A	1.000	3.13	76.8	10	1.99	12.15	11.13	11.38	10.64	11.97	16	20	24	26	LV
659A	1.000	3.13	43.2	30	1.99	12.02	10.40	10.67	9.98	11.20	217	218			S
660A	1.000	3.13	76.8	30	1.99	11.77	10.28	11.64	11.09	11.93	141	142			S
661A	1.000	3.13	43.2	10	2.01	11.34	9.98	11.14	10.62	11.33	4	23	25	27	LV
662A	1.000	3.13	76.8	10	2.01	11.34	10.02	11.31	10.87	11.55	12	13	26	27	LV
663A	1.000	3.13	43.2	30	2.01	13.32	12.09	12.42	11.24	12.53	349				S
664A	1.000	3.13	76.8	30	2.01	11.07	10.06	10.63	10.26	10.74	187	188			S
665A	1.000	3.13	60.0	20	2.00	11.54	10.43	1.71	10.87	12.16	80	100	130	131	LV
666A	1.000	3.13	60.0	20	2.00	12.04	10.21	11.08	10.28	11.66	96	100	219	228	LV
667A	1.000	3.13	60.0	20	2.00	11.50	10.32	11.33	11.17	11.54	254	262	282	283	LV
668A	1.000	3.13	20.0	20	2.00	11.82	10.53	11.51	10.68	11.62	989	990			S
669A	1.000	3.13	100.0	20	2.00	11.23	10.26	10.94	10.70	11.09	48	50	67	68	LV
670A	1.000	3.13	60.0	0	2.00	11.32	10.17	11.35	10.68	11.37	2	3	4	5	LV
671A	1.000	3.13	60.0	40	2.00	11.10	10.11	11.27	10.75	11.27	127	128			S
672A	1.000	3.13	60.0	20	1.98	11.17	10.00	11.14	10.74	11.09	125	126	144	149	LV
673A	1.000	3.13	60.0	20	2.02	11.34	10.04	10.72	10.43	11.33	69	75	103	104	LV
674A	1.625	3.13	43.2	10	1.99	11.33	10.17	11.46	10.51	11.87	35	36	53	54	LV
675A	1.625	3.13	76.8	10	1.99	11.43	10.17	10.62	9.57	11.87	2	3	5	6	LV

TABLE I. - Continued. 12 AMP-HR SILVER-ZINC CHARACTERIZATION TEST

PACK NO.	CHARGE RATE AMPS	DISCHARGE RATE AMPS	DEPTH OF DISCHARGE X	TEST TEMP °C	END OF CHARGE VOLTS	ACTUAL FORMATION CAPACITY					CYCLES TO FAILURE				FAILURE MODE
						CHG#1 A-H	DCHG#1 A-H	CHG#2 A-H	DCHG#2 A-H	CHG#3 A-H	F1	F2	F3	F4	
676A	1.625	3.13	43.2	30	1.99	13.34	12.07	12.38	11.21	12.26	305				S
677A	1.625	3.13	76.8	30	1.99	12.16	10.51	11.64	11.09	12.22	159	160			S
678A	1.625	3.13	43.2	10	2.01	11.88	10.43	11.49	10.51	12.21	43	44	48	70	LV
679A	1.625	3.13	76.8	10	2.01	11.16	10.02	10.98	10.11	10.78	2	3	6	7	LV
680A	1.625	3.13	43.2	30	2.01	11.32	10.11	11.09	10.24	11.16	279	280			S
681A	1.625	3.13	76.8	30	2.00	10.92	9.83	11.20	10.32	11.26	148	149			S
682A	1.625	3.13	60.0	20	2.00	11.63	10.55	11.36	10.62	11.16	15	16	26	106	LV
683A	1.625	3.13	60.0	20	2.00	11.04	9.64	10.87	10.00	10.79	13	14	18	19	LV
684A	1.625	3.13	60.0	20	2.00	11.84	10.55	11.91	10.28	11.99	16	19	22	62	LV
685A	1.625	3.13	20.0	20	2.00	10.89	9.83	11.19	10.40	10.94	335	357	507	508	LV
686A	1.625	3.13	100.0	20	2.00	11.80	10.68	10.82	10.24	10.89	27	28	40	43	LV
687A	1.625	3.13	60.0	0	2.00	11.69	10.38	11.36	10.70	11.75	1	2	3	4	LV
688A	1.625	3.13	60.0	40	2.00	11.03	10.17	11.31	10.92	11.56	90	91			S
689A	1.625	3.13	60.0	20	1.98	13.30	12.13	12.56	11.30	12.56	43	125	135		LV
690A	1.625	3.13	60.0	20	2.02	12.41	11.15	11.17	10.49	12.35	188	189	232	280	LV
691A	0.375	5.00	43.2	10	1.99	12.72	11.66	11.80	10.94	12.56	12	13	21	22	LV
692A	0.375	5.00	76.8	10	1.99	12.55	11.41	11.68	11.09	12.55	10	12	19	20	LV
693A	0.375	5.00	43.2	30	1.99	12.22	11.23	11.71	10.74	12.28	503				S
694A	0.375	5.00	76.8	30	1.99	11.51	10.17	11.38	10.40	11.87	159	161	163	164	LV
695A	0.375	5.00	43.2	10	2.01	12.02	11.04	11.30	10.26	12.04	15	16	22	23	LV
696A	0.375	5.00	76.8	10	2.01	12.02	10.82	11.40	10.87	12.40	10	12	20	21	LV
697A	0.375	5.00	43.2	30	2.01	12.53	11.53	11.71	10.66	11.94	471	472			S
698A	0.375	5.00	76.8	30	2.01	11.82	10.58	11.86	11.07	11.75	160	161	166	167	LV
699A	0.375	5.00	60.0	20	2.00	12.23	11.11	11.42	10.21	11.93	103	105	134	137	LV
700A	0.375	5.00	60.0	20	2.00	11.20	10.26	11.68	11.06	11.97	145	147	172	175	LV

TABLE I. - Concluded. 12 AMP-HR SILVER-ZINC CHARACTERIZATION TEST

PACK NO.	CHARGE RATE AMPS	DISCHARGE RATE AMPS	DEPTH OF DISCHARGE %	TEST TEMP °C	END OF CHARGE VOLTS	ACTUAL FORMATION CAPACITY CHG#1 A-H	DCHG#1 A-H	CHG#2 A-H	DCHG#2 A-H	CHG#3 A-H	CYCLES TO FAILURE F1	F2	F3	F4	FAILURE MODE
701A	0.375	5.00	60.0	20	2.00	11.44	10.19	10.93	10.62	11.39	107	111	138	139	LV
702A	1.000	5.00	43.2	10	1.99	11.88	10.38	11.34	10.57	11.78	3	4	6	7	LV
703A	1.000	5.00	76.8	10	1.99	12.42	10.96	12.36	11.68	12.39	2	3	5	6	LV
704A	1.000	5.00	43.2	30	1.99	12.59	11.22	11.52	10.89	12.12	469	470	490	491	LV
705A	1.000	5.00	76.8	30	1.99	11.93	10.34	11.03	10.32	11.88	385	386			S
706A	1.000	5.00	43.2	10	2.01	11.92	10.38	11.07	10.25	11.98	3	4	8	9	LV
707A	1.000	5.00	76.8	10	2.01	11.27	10.17	11.00	10.10	11.63	2	3	6	7	LV
708A	1.000	5.00	43.2	30	2.01	11.93	10.19	11.15	10.51	11.88	386	387	305	405	LV
709A	1.000	5.00	76.8	30	2.01	11.59	10.13	10.79	10.00	12.02	252	253			S
710A	1.000	5.00	60.0	20	2.00	11.41	10.49	11.10	10.66	12.01	383	384			S
711A	1.000	5.00	60.0	20	2.00	10.94	10.17	11.02	10.51	11.48	308	310	317	318	LV
712A	1.000	5.00	60.0	20	2.00	12.09	10.98	11.91	11.43	12.40	172	175	236	241	LV
713A	1.000	5.00	20.0	20	2.00	11.66	10.83	11.71	11.39	12.16	796	797			S
714A	1.000	5.00	100.0	20	2.00	11.75	10.92	11.70	11.39	12.17	45	47	64	65	LV
715A	1.000	5.00	60.0	0	2.00	11.96	11.07	11.88	11.51	12.58	1	3	4	5	LV
716A	1.000	5.00	60.0	40	2.00	11.56	10.36	11.01	10.77	11.76	175	176	179	182	LV
717A	1.000	5.00	60.0	20	1.98	12.24	11.13	11.19	10.64	12.23	4	5	17	18	LV
718A	1.000	5.00	60.0	20	2.02	13.15	12.02	12.25	11.17	12.56	25		117		LV
719A	1.625	5.00	43.2	10	1.99	12.47	11.36	11.68	11.06	12.33	3	4	7	8	LV
720A	1.625	5.00	76.8	10	1.99	12.41	11.19	11.29	10.79	12.28	2	3	4	5	LV
721A	1.625	5.00	43.2	30	1.99	11.04	9.96	11.30	10.51	11.88	233	234			S
722A	1.625	5.00	76.8	30	1.99	12.36	11.39	11.54	10.77	12.00	2	3	6	7	LV
723A	1.625	5.00	43.2	10	2.01	12.95	11.62	11.17	10.62	12.07	4	5	7	8	LV
724A	1.625	5.00	76.8	10	2.01	13.09	11.87	11.74	10.40	12.00	2	3	7		LV
725A	1.625	5.00	43.2	30	2.01	12.45	1?	11.52	10.98	12.70	292	294	352	353	LV
726A	1.625	5.00	76.8	30	2.01	11.58	10.58	11.61	10.96	12.00	2	3	6	7	LV
727A	1.625	5.00	60.0	20	2.00	12.88	11.60	11.42	10.79	12.29	5	7	56	57	CS
728A	1.625	5.00	60.0	20	2.00	13.16	12.00	11.66	10.49	12.56	6	165	171		LV
729A	1.625	5.00	60.0	20	2.00	12.55	11.38	11.41	10.79	12.51	7	8	12	16	LV

TABLE II. – LEVELS OF CHARGE RATE AND DISCHARGE

RATE INVESTIGATED

Power supply unit	Charge rate (ζ_1)[a] (amps)	Discharge rate (ζ_2)[a] (amps)
1	0.375	1.25
2	1.000	1.25
3	1.625	1.25
4	0.375	3.13
5	1.000	3.13
6	1.625	3.13
7	0.375	5.00
8	1.000	5.00
9	1.625	5.00

[a]As used in equation (1) of text.

TABLE III. – LEVELS OF DEPTH OF DISCHARGE, TEMPERATURE, AND END OF

CHARGE VOLTAGE INVESTIGATED

	DOD_{nom} (%)	$T(\zeta_4)$[a] (°C)	ECV (ζ_5)[a] (volts)
2^3 Factorial Points	43.2	10	1.99
	76.8	10	1.99
	43.2	30	1.99
	76.8	30	1.99
	43.2	10	2.01
	76.8	10	2.01
	43.2	30	2.01
	76.8	30	2.01
Center Points	60.0	20	2.00
	60.0	20	2.00
	60.0	20	2.00
Axial Points	20.0	20	2.00
	100.0	20	2.00
	60.0	0	2.00
	60.0	40	2.00
	60.0	20	1.98
	60.0	20	2.02

[a]As used in equation (1) of text.

TABLE IV. - ESTIMATED COEFFICIENTS OF EQUATION FOR f_2 FAILURE CYCLE USING
ALL THE DATA. REDUCED MODEL USES ONLY THOSE COEFFICIENTS
SIGNIFICANT AT THE 5% LEVEL OF SIGNIFICANCE

Coefficient	Full model Estimate (standard error)	Reduced model Estimate (standard error)	Associated variable
β_0	2.12(0.08)*	2.10(0.06)*	
β_1	-.29(0.04)*	-.28(0.04)*	$X_1 = (CR - 1.0)/0.625$
β_2	-.18(0.04)*	-.18(0.04)*	$X_2 = (DR - 3.13)/1.87$
β_3	-.23(0.03)*	-.23(0.03)*	$X_3 = (DOD - 67.2)/19.4$
β_4	.46(0.03)*	.46(0.03)*	$X_4 = (T - 20)/10$
β_{11}	-.11(0.06)		X_1^2
β_{12}	-.05(0.05)		$X_1 X_2$
β_{22}	-.15(0.06)*	-.15(0.06)*	X_2^2
β_{13}	-.11(0.04)*	-.11(0.04)*	$X_1 X_3$
β_{23}	-.01(0.04)		$X_2 X_3$
β_{33}	.04(0.02)		X_3^2
β_{14}	.06(0.04)		$X_1 X_4$
β_{24}	.17(0.04)*	.18(0.04)*	$X_2 X_4$
β_{34}	.02(0.04)*		$X_3 X_4$
β_{44}	-.20(0.03)*	-.21(0.03)*	X_4^2
Number of data points (n)	127	127	
Standard error of estimate (S)	0.342	0.348	
Squared correlation (R^2)	.789	.771	

(*) Significant at 5% significance level.

TABLE V. - ESTIMATED COEFFICIENTS OF EQUATION FOR f_4 FAILURE CYCLE USING
ALL THE DATA. REDUCED MODEL RETAINS ONLY THOSE COEFFICIENTS
SIGNIFICANT AT THE 5% LEVEL OF SIGNIFICANCE

Coefficient	Full model Estimate (standard error)	Reduced model Estimate (standard error)	Associated variable
β_0	2.25(0.07)*	2.23(0.05)*	
β_1	-.23(0.03)*	-.22(0.03)*	$X_1 = (CR - 1.0)/0.625$
β_2	-.14(0.03)*	-.14(0.03)*	$X_2 = (DR - 3.13)/1.87$
β_3	-.21(0.03)*	-.21(0.03)*	$X_3 = (DOD - 67.2)/19.4$
β_4	.39(0.03)*	.39(0.03)*	$X_4 = (T - 20)/10$
β_{11}	-.08(0.05)		X_1^2
β_{12}	-.05(0.04)		$X_1 X_2$
β_{22}	-.16(0.05)*	-.16(0.05)*	X_2^2
β_{13}	-.09(0.03)*	-.09(0.03)*	$X_1 X_3$
β_{23}	-.01(0.04)		$X_2 X_3$
β_{33}	.03(0.02)		X_3^2
β_{14}	.06(0.04)		$X_1 X_4$
β_{24}	.16(0.04)*	.16(0.04)*	$X_2 X_4$
β_{34}	.01(0.03)		$X_3 X_4$
β_{44}	-.21(0.03)*	-.21(0.02)*	X_4^2
Number of data points (n)	127	127	
Standard error of estimate (S)	0.284	0.287	
Squared correlation (R^2)	.802	.787	

(*) Significant at 5% significance level.

TABLE VI. - ESTIMATED COEFFICIENTS OF EQUATION FOR f_2 FAILURE CYCLE USING
EDITED DATA SET. REDUCED MODEL RETAINS ONLY THOSE COEFFICIENTS
SIGNIFICANT AT THE 5% LEVEL OF SIGNIFICANCE

Coefficient	Full model Estimate (standard error)	Reduced model Estimate (standard error)	Associated variable
β_0	2.08(0.07)*	1.98(0.04)*	
β_1	-.24(0.04)*	-.25(0.04)*	$X_1 = (CR - 1.0)/0.625$
β_2	-.13(0.04)*	-.14(0.04)*	$X_2 = (DR - 3.13)/1.87$
β_3	-.21(0.03)*	-.21(0.03)*	$X_3 = (DOD - 67.2)/19.4$
β_4	.49(0.03)*	.49(0.03)*	$X_4 = (T - 20)/10$
β_{11}	-.05(0.05)		X_1^2
β_{12}	.03(0.05)		$X_1 X_2$
β_{22}	-.10(0.06)		X_2^2
β_{13}	-.07(0.04)*	-.07(0.04)*	$X_1 X_3$
β_{23}	.03(0.04)		$X_2 X_3$
β_{33}	.04(0.02)*	.04(0.02)*	X_3^2
β_{14}	.10(0.04)*	.10(0.04)*	$X_1 X_4$
β_{24}	.21(0.04)*	.21(0.04)*	$X_2 X_4$
β_{34}	.07(0.04)		$X_3 X_4$
β_{44}	-.20(0.03)*	-.20(0.03)*	X_4^2
Number of data points (n)	123	123	
Standard error of estimate (S)	0.296	0.300	
Squared correlation (R^2)	.838	.826	

(*) Significant at the 5% significance level.

TABLE VII. - ESTIMATED COEFFICIENTS OF EQUATION FOR f_4 FAILURE CYCLE USING
EDITED DATA SET. REDUCED MODEL RETAINS ONLY THOSE COEFFICIENTS
SIGNIFICANT AT THE 5% LEVEL OF SIGNIFICANCE

Coefficient	Full Model Estimate (standard error)	Reduced Model Estimate (standard error)	Associated variable
β_0	2.22(0.06)★	2.23(0.04)★	
β_1	-.19(0.03)★	-.19(0.03)★	$X_1 = (CR - 1.0)/0.625$
β_2	-.10(0.03)★	-.10(0.03)★	$X_2 = (DR - 3.13)/1.87$
β_3	-.19(0.02)★	-.19(0.02)★	$X_3 = (DOD - 67.2)/19.4$
β_4	.41(0.02)★	.41(0.02)★	$X_4 = (T - 20)/10$
β_{11}	-.04(0.05)		X_1^2
β_{12}	.02(0.04)		$X_1 X_2$
β_{22}	-.12(0.05)★	-.12(0.05)★	X_2^2
β_{13}	-.05(0.03)★	-.06(0.03)★	$X_1 X_3$
β_{23}	.03(0.03)		$X_2 X_3$
β_{33}	.02(0.02)		X_3^2
β_{14}	.09(0.03)★	.09(0.03)★	$X_1 X_4$
β_{24}	.19(0.03)★	.19(0.03)★	$X_2 X_4$
β_{34}	.05(0.03)		$X_3 X_4$
β_{44}	-.20(0.02)★	-.21(0.02)★	X_4^2
Number of data points (n)	123	123	
Standard error of estimate (S)	0.246	0.248	
Squared correlation (R^2)	.849	.839	

(*) Significant at 5% significance level.

TABLE VIII. - PARAMETERS FOR CANONICAL ANALYSIS OF f_2 FAILURE
CYCLE USING COEFFICIENTS OF FULL MODEL

		j = 1	j = 2	j = 3	j = 4
Components of stationary point (X_s)		-4.67	-2.50	0.50	-1.17
Eigenvalue (λ_j)		0.057	0.001	-0.092	-0.274
Components of eigenvectors (e_{ij})					
	i = 1	-0.21	0.18	0.95	0.16
	i = 2	.67	.58	-.04	.46
	i = 3	-.69	.62	-.30	.19
	i = 4	-.17	-.49	-.09	.85

TABLE IX. - PARAMETERS FOR CANONICAL ANALYSIS OF f_4 FAILURE CYCLE
USING COEFFICIENTS OF FULL MODEL

		j = 1	j = 2	j = 3	j = 4
Components of stationary point (X_s)		-2.24	0.07	1.04	0.68
Eigenvalue (λ_j)		0.032	-0.012	-0.091	-0.269
Components of eigenvectors (e_{ij})					
	i = 1	-0.23	0.15	0.95	0.12
	i = 2	.78	.45	.07	.42
	i = 3	-.56	.71	-.29	.32
	i = 4	-.15	-.52	-.06	.84

TABLE X. - LEAST SQUARES ESTIMATES OF COEFFICIENTS OF EQUATIONS FOR f_2 CYCLES
TILL FAILURE FITTED FOR EACH MODE OF FAILURE

SEPARATELY USING ALL THE DATA

Coefficient	Low voltage failures Estimate (standard error)	Short failures Estimate (standard error)	Associated variable
β_0	2.08(0.07)	2.45(0.10)	
β_1	-.36(0.05)	-.07(0.03)	$X_1 = (CR - 1.0)/0.625$
β_2	-.26(0.05)	-.13(0.03)	$X_2 = (DR - 3.13)/1.87$
β_3	-.25(0.04)	-.10(0.02)	$X_3 = (DOD - 67.2)/19.4$
β_4	.50(0.05)	.003(0.12)[a]	$X_4 = (T - 20)/10$
β_{11}			X_1^2
β_{12}		-.13(0.05)	$X_1 X_2$
β_{22}	-.18(0.08)		X_2^2
β_{13}		-.07(0.03)	$X_1^2 X_3$
β_{23}		.08(0.03)	$X_2 X_3$
β_{33}		.04(0.02)	X_3^2
β_{14}			$X_1 X_4$
β_{24}	.09(0.05)		$X_2 X_4$
β_{34}			$X_3 X_4$
β_{44}	-.16(0.04)	-.11(0.05)	X_4^2
Number of data points (n)	98	29	
Standard error of estimate (S)	0.349	0.095	
Squared correlation (R^2)	.775	.924	

(a) All coefficients significant at 5% significance level except that X_4 is retained regardless of significance.

TABLE XI . - LEAST SQUARES ESTIMATES OF COEFFICIENTS OF EQUATIONS FOR f_4 CYCLES

TILL FAILURE FITTED FOR EACH MODE OF FAILURE SEPARATELY

USING ALL THE DATA   (127 CELLS)

Coefficient	Low voltage failures	Short failures	Associated variable
	Estimate (standard error)	Estimate (standard error)	
β_0	2.24(0.05)	2.44(0.06)	
β_1	-.28(0.04)	-.07(0.03)	$X_1 = (CR - 1.0)/0.625$
β_2	-.20(0.04)	.13(0.03)	$X_2 = (DR - 3.13)/1.87$
β_3	-.23(0.03)	-.11(0.02)	$X_3 = (DOD - 67.2)/19.4$
β_4	.44(0.04)	.03(0.05)[a]	$X_4 = (T - 20)/10$
β_{11}			X_1^2
β_{12}		-.13(0.05)	$X_1 X_2$
β_{22}	-.21(0.06)		X_2^2
β_{13}		-.07(0.03)	$X_1 X_3$
β_{23}		.08(0.03)	$X_2 X_3$
β_{33}		.04(0.02)	X_3^2
β_{14}			$X_1 X_4$
β_{24}	.08(0.04)		$X_2 X_4$
β_{34}			$X_3 X_4$
β_{44}	-.17(0.03)	-.12(0.03)	X_4^2
Number of data points (n)	97	30	
Standard error of estimate (S)	0.287	0.093	
Squared correlation (R^2)	.797	.928	

(a) All coefficients significant at 5% significance level except that X_4 is retained regardless of significance.

TABLE XII. - MAXIMUM LIKELIHOOD ESTIMATES OF COEFFICIENTS OF EQUATIONS FOR f_2 CYCLES TILL FAILURE FITTED FOR EACH MODE OF FAILURE SEPARATELY USING ALL THE DATA (127 CELLS)

Coefficient	Low voltage failures Estimate (standard error)	Short failures Estimate (standard error)	Associated variable
β_0	2.27(0.06)	2.72(0.08)	
β_1	-.28(0.04)	-.09(0.02)	$X_1 = (CR - 1.0)/0.625$
β_2	-.06(0.04)	.14(0.02)	$X_2 = (DR - 3.13)/1.87$
β_3	-.25(0.03)	-.10(0.02)	$X_3 = (DOD - 67.2)/19.4$
β_4	.61(0.05)	-.23(0.09)	$X_4 = (T - 20)/10$
β_{11}			X_1^2
β_{12}		-.11(0.03)	$X_1 X_2$
β_{22}	-.11(0.06)		X_2^2
β_{13}		-.08(0.02)	$X_1 X_3$
β_{23}		.07(0.02)	$X_2 X_3$
β_{33}		.00(0.02)	X_3^2
β_{14}			$X_1 X_4$
β_{24}	.18(0.05)		$X_2 X_4$
β_{34}			$X_3 X_4$
β_{44}	-.13(0.02)	.05(0.03)	X_4^2
σ	0.30(0.02)	0.067(0.01)	

TABLE XIII. - MAXIMUM LIKELIHOOD ESTIMATES OF COEFFICIENTS OF EQUATIONS FOR f_4 CYCLES TILL FAILURE FITTED FOR EACH MODE OF FAILURE SEPARATELY USING ALL THE DATA

Coefficient	Low voltage failures Estimate (standard error)	Short failures Estimate (standard error)	Associated variable
β_0	2.37(0.05)	2.68(0.06)	
β_1	-.23(0.04)	-.07(0.02)	$X_1 = (CR - 1.0)/0.625$
β_2	-.05(0.03)	.14(0.02)	$X_2 = (DR - 3.13)/1.87$
β_3	-.23(0.02)	-.11(0.02)	$X_3 = (DOD - 67.2)/19.4$
β_4	.51(0.04)	-.12(0.07)	$X_4 = (T - 20)/10$
β_{11}			X_1^2
β_{12}		.10(0.04)	$X_1 X_2$
β_{22}	-.13(0.05)		X_2^2
β_{13}		-.09(0.02)	$X_1 X_3$
β_{23}		.07(0.02)	$X_2 X_3$
β_{33}		-.01(0.01)	X_3^2
β_{14}			$X_1 X_4$
β_{24}	.16(0.04)		$X_2 X_4$
β_{34}			$X_3 X_4$
β_{44}	-.14(0.03)	-.09(0.03)	X_4^2
σ	0.25(0.02)	0.08(0.01)	

TABLE XIV. - LEAST SQUARES ESTIMATES OF COEFFICIENTS OF EQUATIONS FOR f_2 CYCLES TILL FAILURE FITTED FOR EACH MODE OF FAILURE SEPARATELY USING EDITED DATA SET

Coefficient	Low voltage failures Estimate (standard error)	Short failures Estimate (standard error)	Associated variable
β_0	2.09(0.06)	2.46(0.09)	
β_1	-.31(0.04)	-.09(0.03)	$X_1 = (CR - 1.0)/0.625$
β_2	-.20(0.04)	.12(0.03)	$X_2 = (DR - 3.13)/1.87$
β_3	-.23(0.03)	-.09(0.02)	$X_3 = (DOD - 67.2)/19.4$
β_4	.55(0.05)	.00(0.11)[a]	$X_4 = (T - 20)/10$
β_{11}			X_1^2
β_{12}		-.11(0.05)	$X_1 X_2$
β_{22}	-.16(0.07)		X_2^2
β_{13}		-.08(0.03)	$X_1 X_3$
β_{23}		.07(0.03)	$X_2 X_3$
β_{33}		.04(0.02)	X_3^2
β_{14}			$X_1 X_4$
β_{24}	.15(0.05)		$X_2 X_4$
β_{34}			$X_3 X_4$
β_{44}	-.15(0.04)	-.11(0.04)	X_4^2
Number of data points (n)	95	28	
Standard error or estimate (S)	0.308	0.101	
Squared correlation (R^2)	.815	.900	

(a) All coefficients significant at 5% significance level except that X_4 is retained regardless of significance.

TABLE XV. - LEASE SQUARES ESTIMATES OF COEFFICIENTS OF EQUATIONS FOR f_4 CYCLES

TILL FAILURE FITTED FOR EACH MODE OF FAILURE SEPARATELY

USING EDITED DATA SET

Coefficient	Low voltage failure Estimate (standard error)	Short failure Estimate (standard error)	Associated variable
β_0	2.24(0.05)	2.46(0.09)	
β_1	-.24(0.03)	-.09(0.03)	$X_1 = (CR - 1.0)/0.625$
β_2	-.16(0.03)	.12(0.03)	$X_2 = (DR - 3.13)/1.87$
β_3	-.21(0.03)	-.09(0.02)	$X_3 = (DOD - 67.2)/19.4$
β_4	.47(0.04)	.00(0.11)[a]	$X_4 = (T - 20)/10$
β_{11}			X_1^2
β_{12}		-.11(0.05)	X_1X_2
β_{22}	-.19(0.06)		X_2^2
β_{13}		-.08(0.03)	X_1X_3
β_{23}		.07(0.03)	X_2X_3
β_{33}		.04(0.02)	X_3^2
β_{14}			X_1X_4
β_{24}	.13(0.04)		X_2X_4
β_{34}			X_3X_4
β_{44}	-.16(0.03)	-.11(0.04)	X_4^2
Number of data points (n)	95	28	
Standard error of estimate (S)	0.253	0.101	
Squared correlation (R^2)	.838	.900	

(a) All coefficients significant at 5% significance level except that X_4 is retained regardless of significance.

TABLE XVI. - MAXIMUM LIKELIHOOD ESTIMATES OF COEFFICIENTS OF EQUATIONS

FOR f_2 CYCLES TILL FAILURE FITTED FOR EACH MODE OF

FAILURE SEPARATELY USING EDITED DATA SET

Coefficient	Low voltage failures	Short failures	Associated variable
	Estimate (standard error)	Estimate (standard error)	
β_0	2.27(0.05)	2.70(0.07)	
β_1	-.25(0.04)	-.09(0.02)	$X_1 = (CR - 1.0)/0.625$
β_2	-.03(0.04)	.14(0.02)	$X_2 = (DR - 3.13)/1.87$
β_3	-.25(0.03)	-.09(0.02)	$X_3 = (DOD - 67.2)/19.4$
β_4	.63(0.05)	-.20(0.08)	$X_4 = (T - 20)/10$
β_{11}			X_1^2
β_{12}		-.09(0.02)	X_1X_2
β_{22}	-.10(0.06)		X_2^2
β_{13}		-.09(0.02)	X_1X_3
β_{23}		.06(0.02)	X_2X_3
β_{33}		.01(0.02)	X_3^2
β_{14}			X_1X_4
β_{24}	.19(0.05)		X_2X_4
β_{34}			X_3X_4
β_{44}	-.13(0.04)	-.05(0.03)	X_4^2
σ	0.28(0.02)	0.062(0.01)	

TABLE XVII. - MAXIMUM LIKELIHOOD ESTIMATES OF COEFFICIENTS OF EQUATIONS
FOR f_4 CYCLES TILL FAILURE FITTED FOR EACH MODE OF FAILURE
SEPARATELY USING EDITED DATA SHEET

Coefficient	Low voltage failures	Short failures	Associated variable
	Estimate (standard error)	Estimate (standard error)	
β_0	2.37(0.04)	2.74(0.07)	
β_1	-.21(0.03)	-.09(0.02)	$X_1 = (CR - 1.0)/0.625$
β_2	-.02(0.03)	.14(0.02)	$X_2 = (DR - 3.13)/1.87$
β_3	-.23(0.02)	-.10(0.02)	$X_3 = (DOD - 67.2)/19.4$
β_4	.52(0.04)	-.22(0.09)	$X_4 = (T - 20)/10$
β_{11}			X_1^2
β_{12}		-.08(0.03)	X_1X_2
β_{22}	-.12(0.05)		X_2^2
β_{13}		-.09(0.02)	X_1X_3
β_{23}		.06(0.02)	X_2X_3
β_{33}		.00(0.02)	X_3^2
β_{14}			X_1X_4
β_{24}	.16(0.04)		X_2X_4
β_{34}			X_3X_4
β_{44}	-.14(0.03)	-.05(0.03)	X_4^2
σ	0.23(0.02)	0.066(0.01)	

Figure 1. – Predicted cycles until I_2 failure vs actual depth of discharge for five temperatures. Data from reduced model coefficients of Table VI. Charge rate of 1.0 amp, discharge rate of 3.13 amp, and end charge voltage of 2.00 volts.
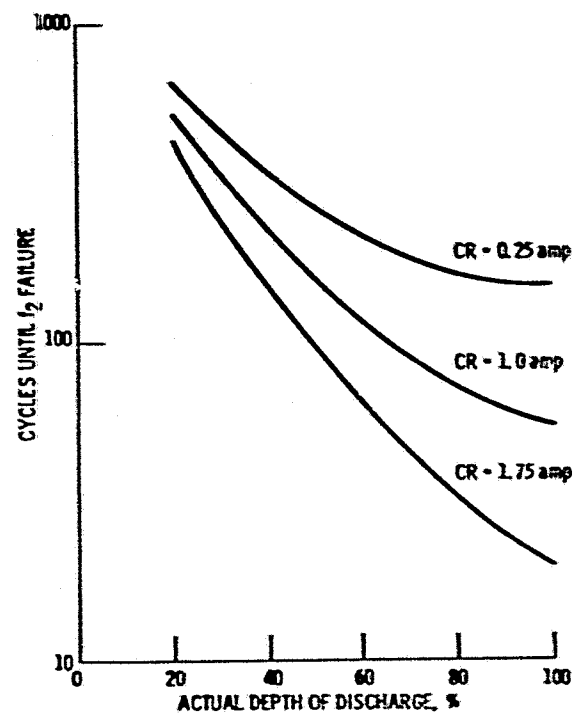
Figure 2. – Predicted cycles until I_2 failure vs actual depth of discharge for three charge rates. Data from full model coefficients of Table VI. Temperature of 20^0 C, discharge rate of 3.13 amp, end of discharge voltage of 2.00 volts.
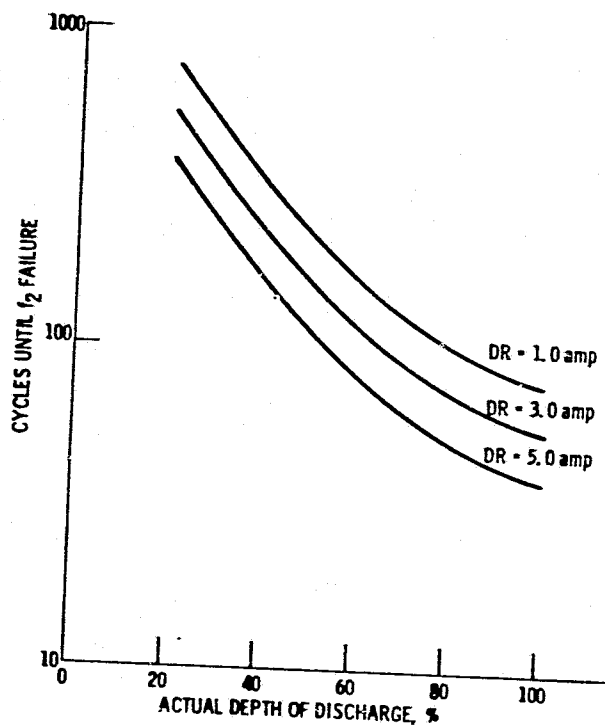
Figure 3. - Predicted cycles until f_2 failure vs actual depth of discharge for three discharge rates. Data from full model coefficients of Table VI. Charge rate of 1.0 amp, temperature of 20° C, end of charge voltage of 2.00 volts.
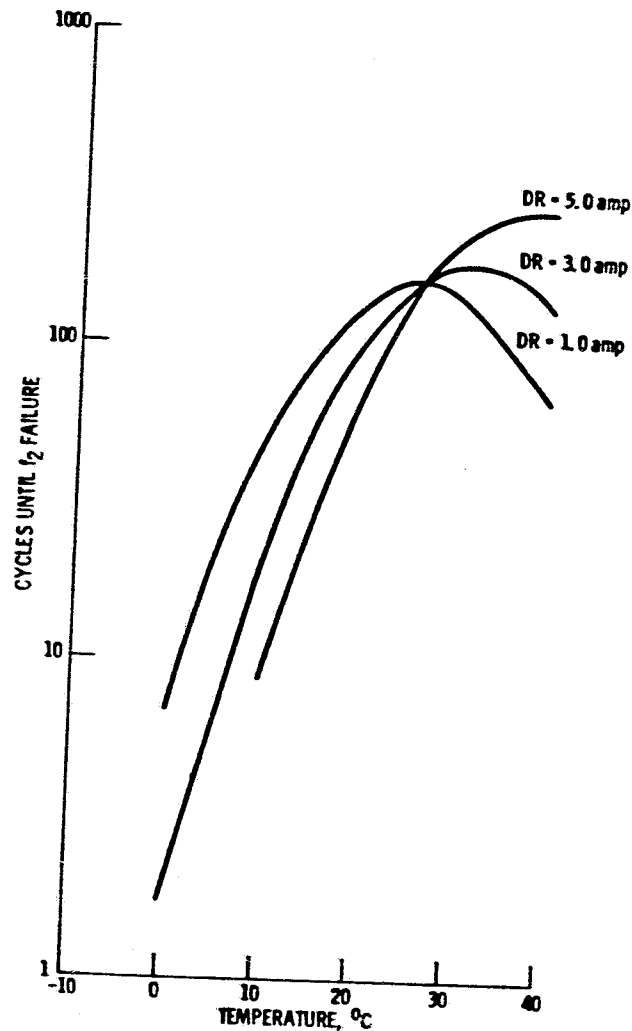
Figure 4. - Predicted cycles until f_2 failure vs temperature for three discharge rates. Data from reduced model coefficients of Table VI. Uses charge rate of 1.0 amp, actual depth of discharge of 67.2%, end of charge voltage of 2.00 volts.
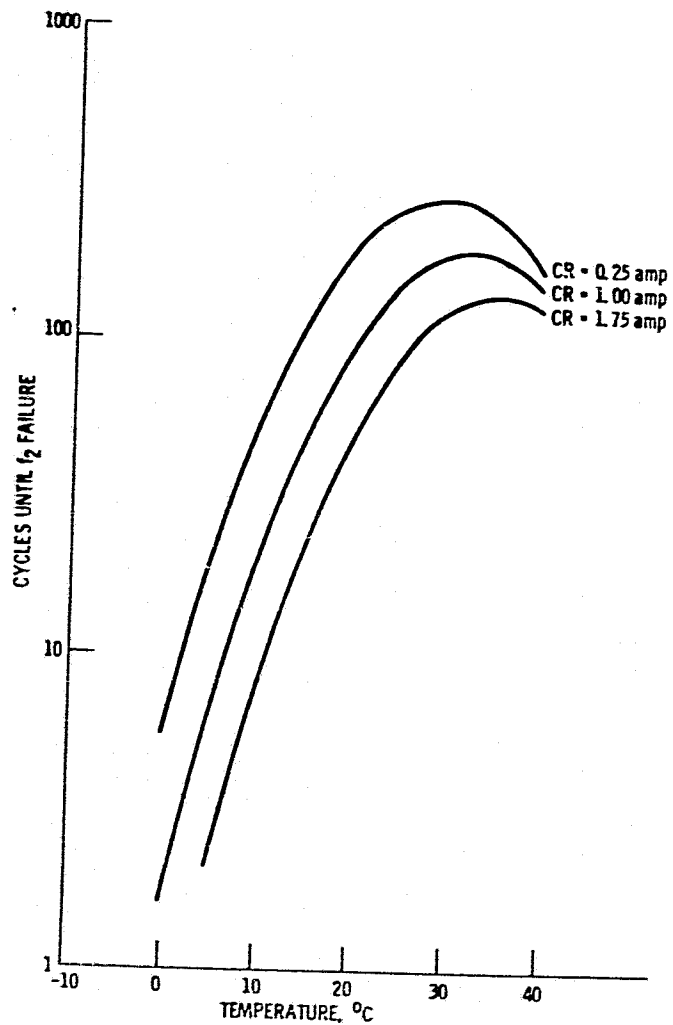
Figure 5. – Predicted cycles until f_2 failure vs temperature for three charge rates. Data from coefficients of reduced model of Table VL. Discharge rate is 3.13 amp, actual depth of discharge is 67.2%, and end of charge voltage is 2.00 volts.
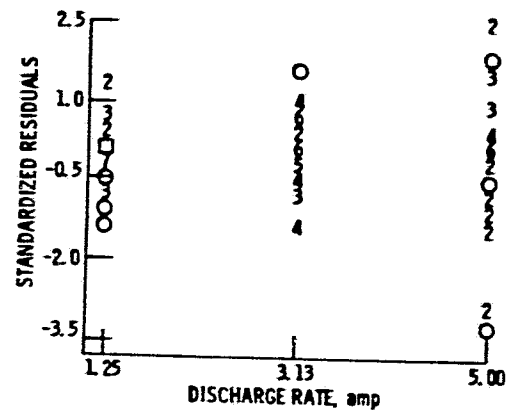
Figure 6. – Standardized residuals from predicted equation using least squares for cycles until low voltage f_2 failure. (Data based on reduced model of Table X.) Standardized residuals defined as $(y_i - \bar{y}_i)$vs. Symbols plotted indicate number of points observed at those co-ordinates (O denotes a single value, 2 through 9 indicates that many values, □ indicates 10 or more).
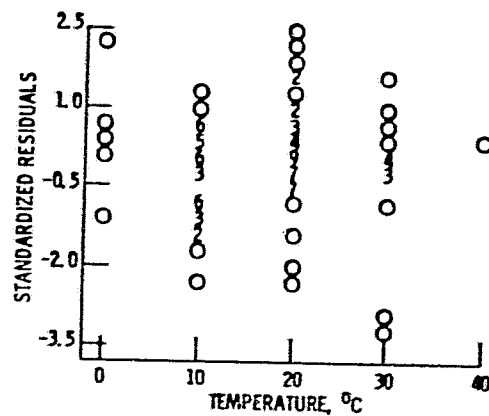

Figure 7. – Standardized residuals from predicted equation for cycles until low voltage f_v failure. (Data based on reduced equation of Table X.) Standardized residuals defined as $(y_i - \bar{y}_i)$vs. Symbols plotted indicate number of points observed at those co-ordinates (O denotes a single value, 2 through 9 indicates that many variables, □ indicates 10 or more).
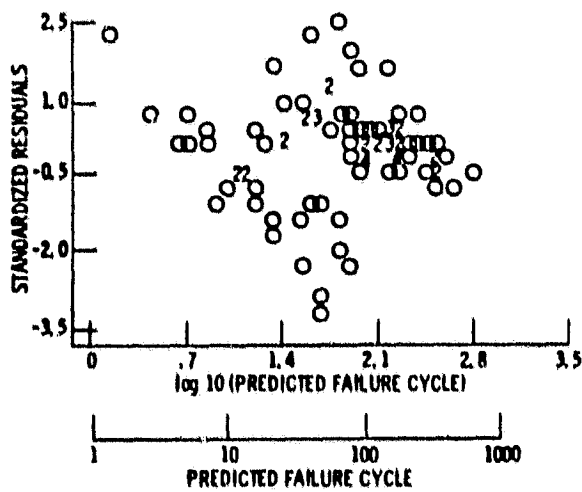
Figure 8. - Standardized residuals from predicted equation using least squares for cycles until low voltage f_v failures. (Data based on coefficients of Table XI.) Standardized residuals defined as $(y - \hat{y})/s$. Symbols plotted indicate number of points observed at those co-ordinates ($\bigcirc$ denotes a single value, 2 through 9 indicates that many values, $\square$ indicates 10 or more).
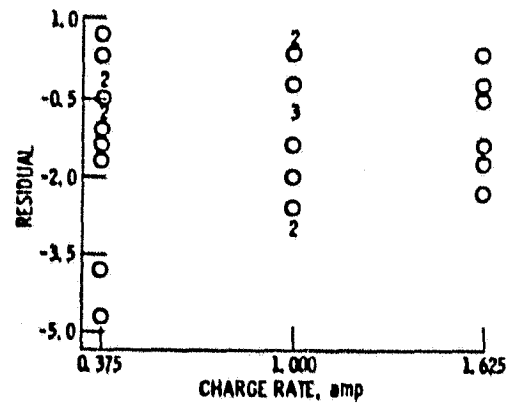
Figure 9. - Residuals vs charge rate from the maximum likelihood estimates for the f_4 shorting failures. (Data based on all the data and coefficients of Table XIII.) Residuals defined as observed $\log_{10}$ (f_4 short failure cycle) minus estimated location parameter of extreme value distribution. Symbols plotted indicate number of points observed at those co-oridinates ($\bigcirc$ denotes a single value, 2 through 9 indicates that many points).
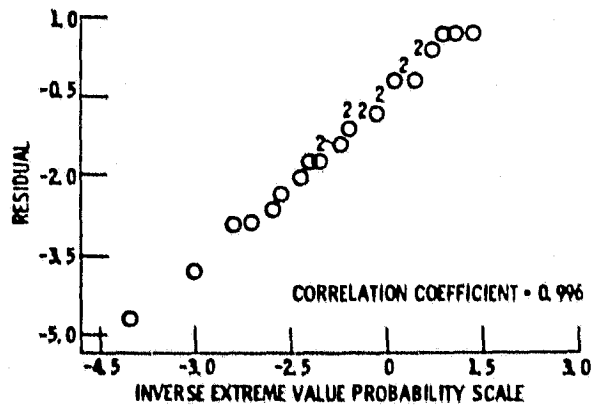
Figure 10. - Probability plot of residuals from maximum likelihood fit of cycles until f_4 short failure using all the data plotted using extreme value probability scale. Symbols plotted indicate number of points observed at those coordinates ($\bigcirc$ denotes a single value, 2 through 9 indicates that many points).
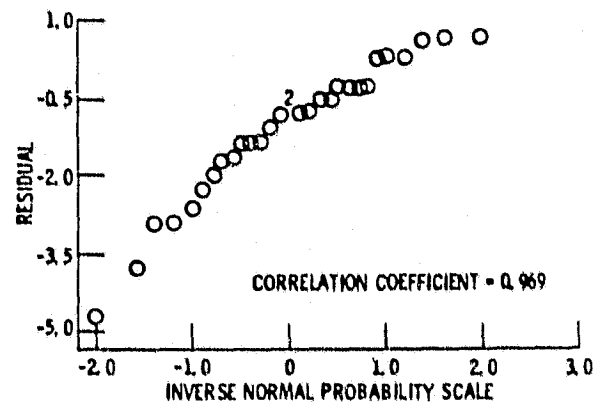
Figure 11. - Probability plot of residuals from maximum likelihood fit of cycles until f_4 short failure using all the data plotted using normal probability scale. Symbols plotted indicate number of points observed at those coordinates ($\bigcirc$ denotes a single value, 2 through 9 indicates that many points).
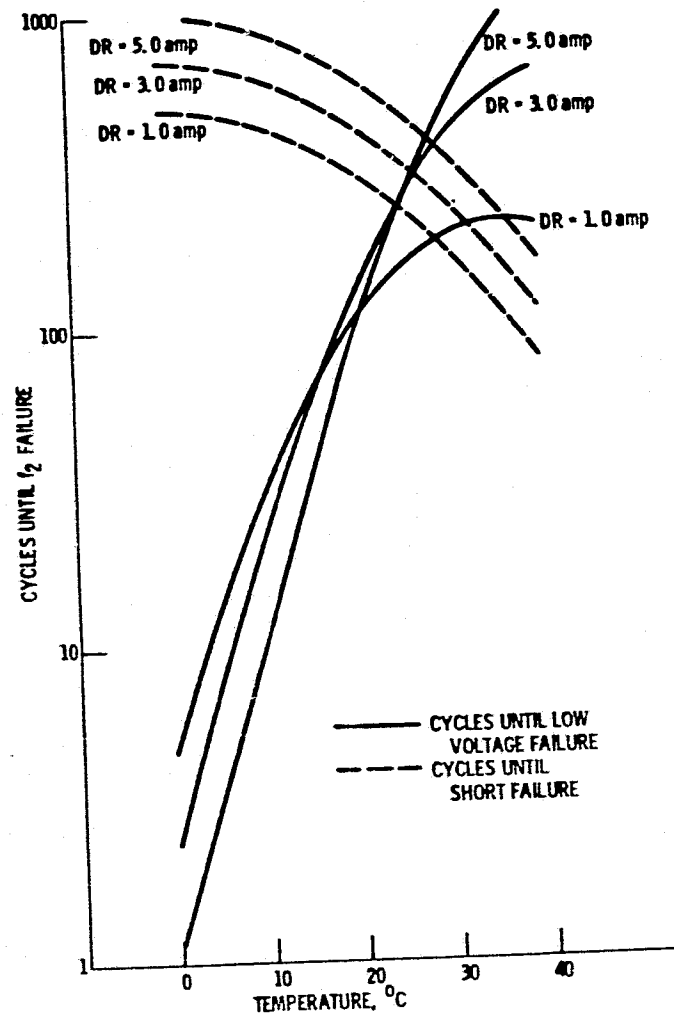
Figure 12. - Expected cycles until f_2 failure for each mode separately vs temperature for three discharge rates. Data based on coefficients given in Table XVI. Uses charge rate of 1.0 amp, actual depth of discharge of 67.2% and end of charge voltage of 2.00 volts.
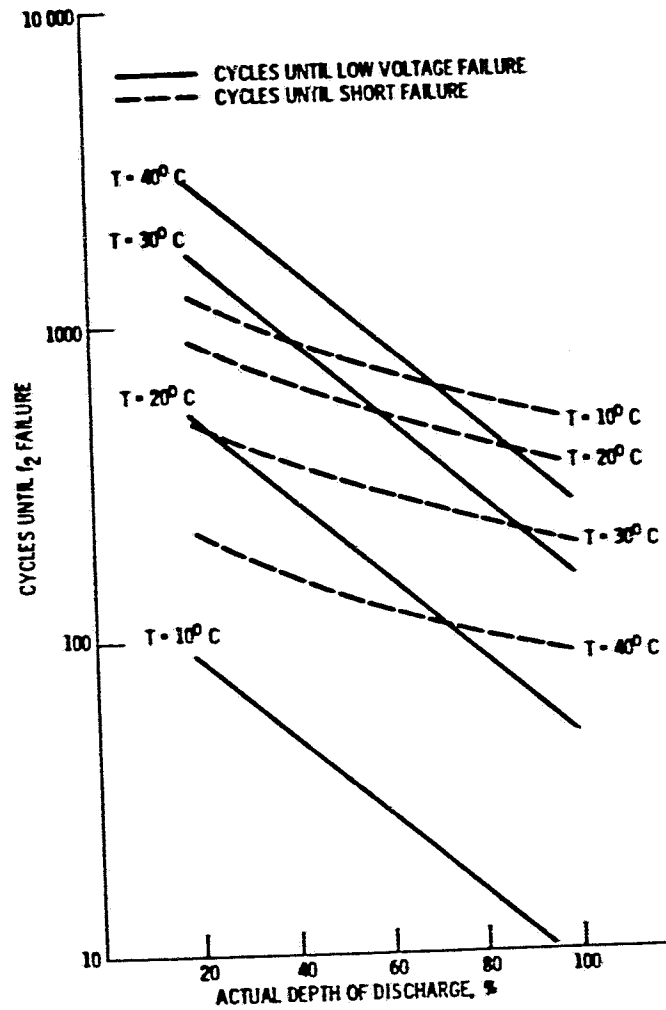

Figure 13. - Expected cycles until f_2 failure for each mode separately vs actual depth of discharge for four temperatures. Data based on coefficients of Table XVI. Uses charge rate of 1.0 amp, discharge rate of 3.15 amp, and end of charge voltage of 2.00 volts.
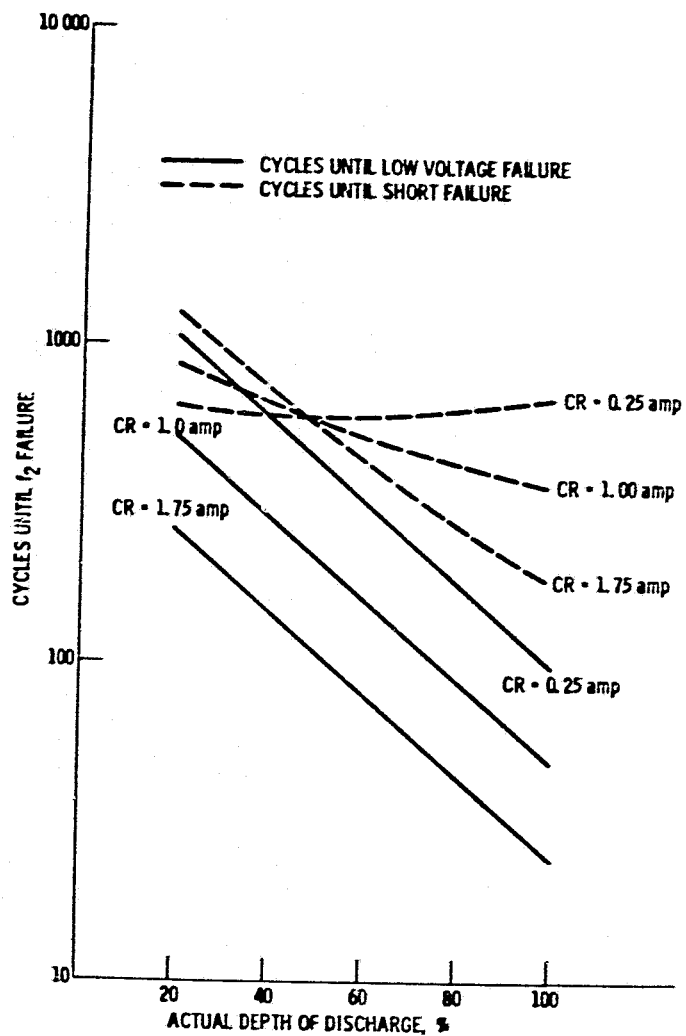
Figure 14. - Expected cycles until f_2 failure for each mode separately as a function of actual depth of discharge for three charge rates. Data based on coefficients of Table XVI. Uses discharge rate of 3.? amp, temperature of 20° C, and end of charge voltage of .0 volts.
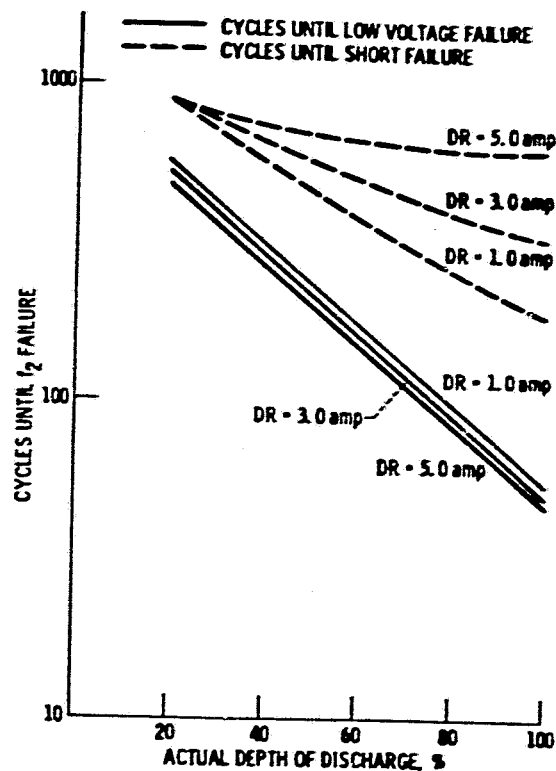

Figure 15. - Expected cycles until f_2 failure for each mode separately as a function of actual depth of discharge for three discharge rates. Data based on coefficients of Table XVI. Uses charge rate of 1.0 amp, temperature of 20° C, and end of charge voltage of 2.00 volts.
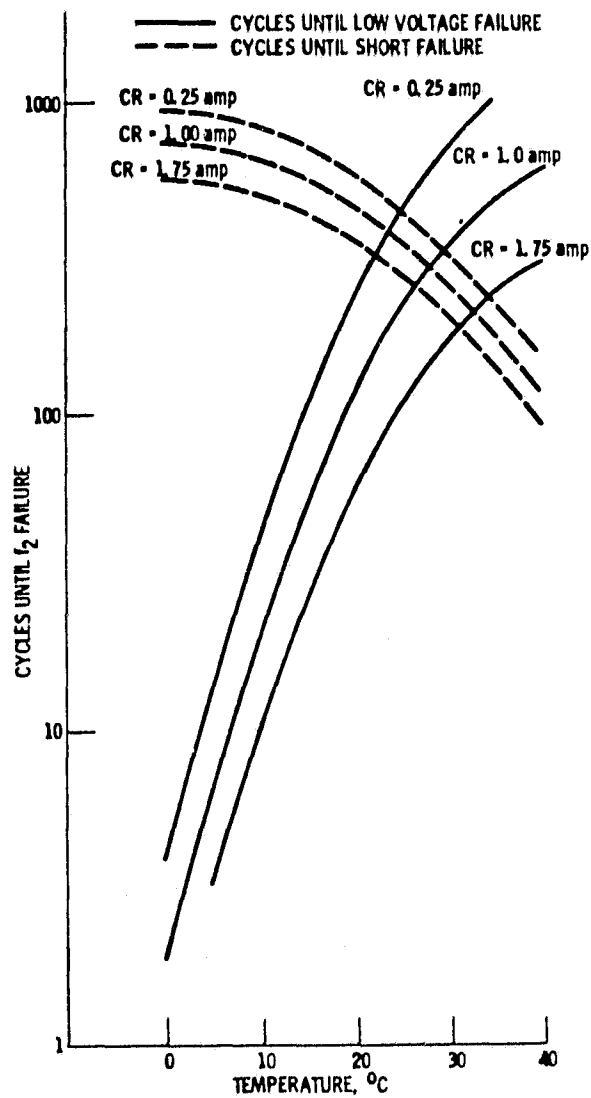
Figure 16. - Expected cycles until f_2 failure for each mode separately as a function of temperature for three charge rates. Data based on coefficients of Table XVI. Uses actual discharge rate of 3.13 amp, depth of discharge of 67.2%, and end of charge voltage of 2.00 volts.